Modeling Carbon Nanostructures with Empirical Interatomic Potentials

by
Sophia Thiele

A Dissertation
Submitted to the Department of Materials Science and Technology
of the University of Crete

October 2022

Table of Contents

Acknowledgements

Firstly, I'd like to express my thanks to my thesis supervisor and teacher Professor Georgios Kopidakis for the suggestion of the subject and for his consistent support and guidance during the running of this project. I would also like to thank Georgios Vailakis for providing advice regarding analysis. Without this, the research would not have been possible. Furthermore I would like to thank the rest of the Quantum Theory of Materials Group (QTM) who have been a great source of support. Finally, I would like to thank Professor Stamatis Stamatiadis for helping with this research project.

Περίληψη

Τα υλικά και οι νανοδομές με βάση τον άνθρακα αποτελούν σημαντικό μέρος της επιστημονικής έρευνας. Ο άνθρακας είναι πανταχού παρών στη φύση, από τους ζωντανούς οργανισμούς, οι οποίοι βασίζονται σε οργανικές ενώσεις, μέχρι το σύμπαν, όπου είναι το τέταρτο πιο άφθονο στοιχείο. Τα άτομά του έχουν την ικανότητα να σχηματίζουν ποικίλους δεσμούς με αποτέλεσμα τη δημιουργία διάφορων αλλότροπων, οι οποίες διαδραματίζουν επίσης κρίσιμο ρόλο στην επιστήμη και τη μηχανική των υλικών. Η κατανόηση και η προσομοίωση πολλών διαφορετικών δεσμικών περιβαλλόντων αποτελεί πρόκληση για τη θεωρία και τους υπολογισμούς και σημαντική προσπάθεια επικεντρώθηκε στην ανάπτυξη αξιόπιστων και μεταβιβάσιμων δια-ατομικών δυναμικών για κλασικές προσομοιώσεις μοριακής δυναμικής (ΜΔ). Η παρούσα διατριβή αφορά την εφαρμογή της κλασικής ΜΔ με τη χρήση τέτοιων εμπειρικών δυναμικών για τη δημιουργία υλικών και μορίων που αποτελούνται από άνθρακα και υδρογόνο, τον προσδιορισμό των βασικών δομικών και δυναμικών ιδιοτήτων τους και τη σύγκριση των αποτελεσμάτων με άλλες θεωρητικές μεθόδους, όπως η θεωρία συναρτησιακού πυκνότητας και ισχυρής δέσμευσης, καθώς και με το πείραμα. Πιο συγκεκριμένα, η δομή, τα μήκη δεσμών και τα φάσματα δονήσεων για το διαμάντι, το γραφένιο και τις νανοταινίες του, το μεθάνιο, το βενζόλιο και τις αλυσίδες υδρογονανθράκων εξετάστηκαν με προσομοιώσεις ΜΔ χρησιμοποιώντας δια-ατομικά δυναμικά τάξης δεσμών. Για τις ΜΔ χρησιμοποιήθηκε το πακέτο προσομοίωσης LAMMPS (Large-scale Atomic/Molecular Massively Parallel Simulator) και αναπτύχθηκε εσωτερικό λογισμικό για τον υπολογισμό των δονητικών φασμάτων από τα αποτελέσματα των προσομοιώσεων ΜΔ με χρήση Fast Fourier Transform. Η συστηματική σύγκριση των αποτελεσμάτων δείχνει συνολική συμφωνία μεταξύ των εμπειρικών δυναμικών και του πειράματος, με πολύ λίγες εξαιρέσεις, όπου θα πρέπει να χρησιμοποιούνται ακριβέστερες μέθοδοι πρώτων αρχών. Επιπλέον, τα δονητικά φάσματα αναλύονται ως προς τη θερμοκρασία, τους κανονικούς τρόπους ταλάντωσης και τις εντοπισμένες διεγέρσεις.

Abstract

Carbon based materials and nanostructures are an important part of scientific research. Carbon is ubiquitous in nature, from the living organisms, which are all based on organic compounds, to the universe, where it is the fourth most abundant element. Its atoms have the ability to form diverse bonds resulting in various allotropes which also play a crucial role in materials science and engineering. Understanding and simulating several different bonding environments is a challenge for theory and computation and considerable effort focused on developing reliable and transferrable interatomic potentials for classical molecular dynamics (MD) simulations. This thesis pertains to the application of classical MD using such empirical potentials to create materials and molecules consisting of carbon and hydrogen, determine their basic structural and dynamical properties, and compare the results with other theoretical methods, such as density functional theory and tight-binding, as well as experiment. More specifically, structure, bond lengths and vibrational spectra for diamond, graphene and its nanoribbons, methane, benzene and hydrocarbon chains were examined with MD simulations using bond order interatomic potentials. The simulation package LAMMPS (Large-scale Atomic/Molecular Massively Parallel Simulator) was used for the MD and in-house software was developed for the calculation of vibrational spectra from the results of MD simulations using Fast Fourier Transform. Systematic comparison of results shows overall agreement between empirical potentials and experiment, with very few exceptions, where more accurate first principles methods should be used. Moreover, vibrational spectra are analyzed in terms of temperature, normal modes, and localized excitations.

Chapter 1: Introduction: Carbon Structures

1.1Carbon and its Allotropes

Element: Carbon

Carbon, the 6th element in the periodic table is denoted by letter 'C.' Carbon is found almost everywhere, and it is one of the most abundant materials on earth. It is the 4th most common element in the universe and 15th most common on earth's crust. The name carbon comes from a Latin word "carbo," which means coal and charcoal; hence, it is also derived from the French word "charbon" which means charcoal. Carbon is the building block of life and its uses have shaped human history, from fossil fuels to the diamond trade. Today, carbon once again promises revolutionary applications, thanks to the discovery of nanoscale carbon structures over the past three decades. Carbon's ability to form bonds with four other atoms goes back to its number and configuration of electrons. Carbon has an atomic number of six (meaning six protons, and six electrons as well in a neutral atom), so the first two electrons fill the inner shell and the remaining four are left in the second shell, which is the valence shell. To achieve stability, carbon must find four more electrons to fill its outer shell, giving a total of eight and satisfying the octet rule. Carbon atoms may thus form bonds to as many as four other atoms. For example, in methane (CH_4), carbon forms covalent bonds with four hydrogen atoms. Each bond corresponds to a pair of shared electrons (one from carbon and one from hydrogen), giving carbon the eight electrons it needs for a full outer shell. The molecular binding behavior of carbon is not based on identical molecular orbitals but on hybridization.

Hybridization was introduced to explain molecular structure when the valence bond theory failed to properly calculate them. Valence bond (VB) theory assumes that all bonds are localized bonds formed between two atoms by the donation of an electron from each atom. This is actually an unacceptable statement as many atoms bond using delocalized electrons. It is experimentally observed that bond angles in organic compounds are close to 109,5°, 120°, or 180°. According to Valence Shell Electron Pair Repulsion (VSEPR) theory, electron pairs repel each other and the bonds and lone pairs around a central atom are generally separated by the largest possible angles. [23]

Specifically for the carbon element, in the ground state, there are two unpaired electrons in the outer shell (electron configuration: $(1s)^2(2s)^2(2p)^2$), so that one could assume the ability to bind only two additional molecules. But a binding ability for four electrons is noticed. The reason is the small energy difference between the 2s- and the 2p-state, so that it is easily possible to excite one electron from the 2s-state into the 2p-state. In the presence of an external perturbation, such as a close hydrogen, the energy difference is overcome. This results in a mixed state formed out of one s-orbital and three p-orbitals, namely px, py and pz, is produced. Four new hybrid orbitals are formed. So when carbon is bonded to four other atoms (with no lone

electron pairs), the hybridization is sp^3 and the arrangement is tetrahedral with the center of masses to be in the corners. The characteristic angle between the hybrid orbitals in sp^3-configuration is 109.5 degree. On the other side, a carbon atom bound to three atoms (two single bonds, one double bond) is sp^2 hybridized and forms a flat trigonal or triangular arrangement with 120° angles between bonds. In particular, the sp^2-hybridization is the combination of one s-orbital with only two p-orbitals, namely px and py. The additional pz-orbital is perpendicular to the sp^2-hybrid orbitals and forms a π-bond. The third possible arrangement for carbon is sp hybridization in which the s orbital of the excited state carbon is mixed with only one out of the three 2p orbitals. This hybridization results in a linear arrangement with an angle of 180° between bonds. [23][26]

Allotropy in Carbon

One of the most amazing properties of carbon is its ability to make long carbon chains and rings. This property of carbon is known as catenation. Carbon has many special abilities out of all one unique ability is that carbon forms double or triple bonds with itself and with other electronegative atoms like oxygen and nitrogen. These two properties of carbon i.e catenation and multiple bond formation, it has the number of allotropic forms. Allotrope is nothing but the existence of an element in many forms which will have different physical properties but will have similar chemical properties and its forms are called allotropes of allotropic forms. Carbon allotropes are all based on carbon atoms but exhibit different physical properties, especially with regard to hardness. Carbon exists in two allotropic form (i) crystalline (ii) amorphous.[29] The crystalline forms are diamond and graphite whereas the amorphous forms are coal, charcoal, lamp black etc. Though these allotropes of carbon have a different crystal structure and different physical properties, their chemical properties are similar and show similar chemical properties. Both give off carbon dioxide when strongly heated in the presence of oxygen.

1.2 Graphene, Graphene Nanoribbons and Diamond

Graphene

Graphene is composed of sp^2 hybridized carbon atoms arranged in a 2D honeycomb crystal lattice. Three valence electrons of carbon atoms in graphene form bonds (σ) with their next neighbours while the fourth electron of each carbon atom localized in the pz (π) orbitals perpendicular to the planar sheet form highly delocalized bonds (π) with the others. The name is derived from "graphite" and the suffix -ene, reflects the fact that the graphite allotrope of carbon contains numerous double bonds. In 2004, the material was rediscovered, isolated and investigated at the University of Manchester, by Andre Geim and Konstantin Novoselov. In 2010, Geim and Novoselov were awarded the Nobel Prize in Physics for their "groundbreaking experiments regarding the two-dimensional material graphene". High-quality graphene proved to be surprisingly easy to isolate. [1]

The possibility of wrapping up graphene into 0D fullerenes, rolling it into 1D carbon nanotubes (CNTs) and stacking of it into 3D graphite makes graphene the central building block of all graphitic materials. (see Figure 1.2.1) [2]

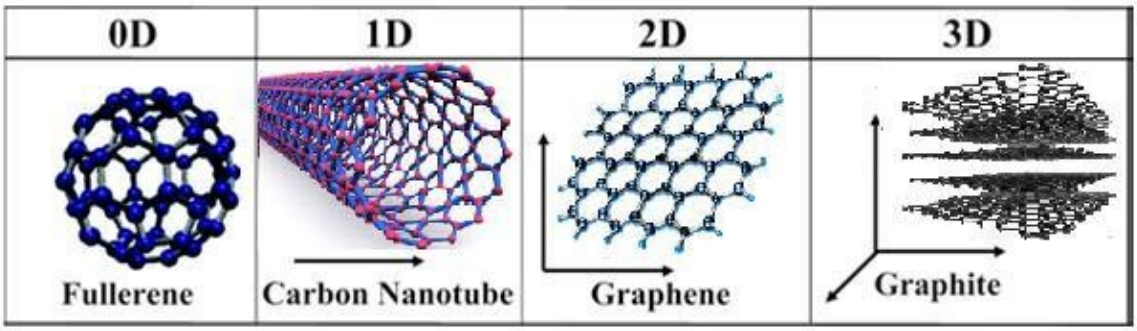

Figure 1.2.1 [2]: examples of different carbon nanostructures: fullerene (0D), carbon nanotubes (1D), graphene (2D), graphite (3D)

Graphene Nanoribbons

Graphene nanoribbons (GNRs) are planar, finite, quasi-one-dimensional graphene structures. They are generally categorized by the structure of their long edges, which can have an armchair, a zigzag, or an intermediate character (see Fig. 1.2.2). [18]. Zigzag GNRs are always metallic, while armchair GNRs can be either metallic or semiconducting. [19]

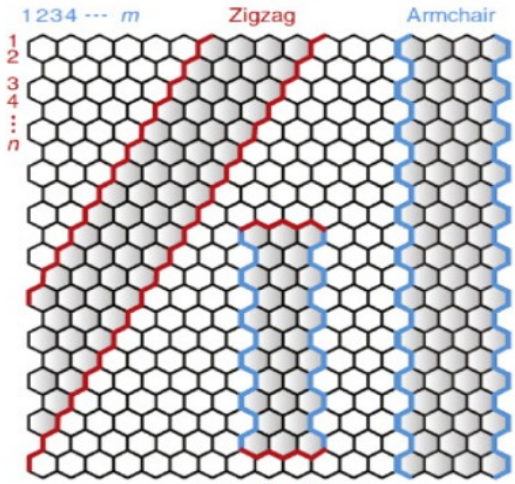

Figure 1.2.2 [18]: Categorization of graphene nanoribbons

Diamond

Diamond is a solid form of the element carbon with its atoms arranged in a crystal structure called diamond cubic. Diamond has the highest hardness and thermal conductivity of any natural material, properties that are used in major industrial applications such as cutting and polishing tools. Although diamond is not fragile or prone to breaking apart, all substances including diamond can fracture or shatter. Due

to its particular crystal structure, diamond has certain planes of weakness along which it can be split. Diamond is said to have perfect cleavage in four different directions, meaning it will separate neatly along these lines rather than in a jagged or irregular fashion. This is because the diamond crystal has fewer chemical bonds along the plane of its octahedral face than in other directions. Diamond cutters take advantage of cleavage to fashion diamonds efficiently. [22] They are also naturally lipophilic and hydrophobic, which means the diamonds' surface cannot be wet by water, but can be easily wet and stuck by oil. [4]

1.3 Forms of Hydrocarbons

Hydrocarbon molecules

Methane, an outstanding fuel, is a good example of hydrocarbons. These are organic molecules consisting completely of carbon and hydrogen and are often used as fuels: the propane in a gas grill or the butane in a lighter. The atoms in hydrocarbons have bonds between them called covalent bonds. This is a type of chemical bond where two atoms are connected to each other by the sharing of two or more electrons. Because hydrocarbons have many such bonds, a large amount of energy is stored, which is released when these molecules are burned (oxidized). Methane is the simplest hydrocarbon molecule, with a central carbon atom bonded to four different hydrogen atoms. The geometry of the methane molecule, where the atoms reside in three dimensions, is determined by the shape of its electron orbitals. The carbon and the four hydrogen atoms form a shape known as a tetrahedron, with four triangular faces; for this reason, methane is described as having tetrahedral geometry. [3]

Hydrocarbon chains

Hydrocarbon chains are formed by successive bonds between carbon atoms and may be branched or unbranched. The whole geometry of the molecule is transformed by the different geometries of single, double, and triple covalent bonds. Double and triple bonds change the geometry of the molecule: single bonds allow rotation along the axis of the bond, while double bonds lead to a planar configuration and triple bonds to a linear one. These geometries have an important impact on the form a particular molecule can assume. [3]

Hydrocarbon rings

The hydrocarbons discussed so far have been aliphatic hydrocarbons, which consist of linear chains of carbon atoms. A different type of hydrocarbon, aromatic hydrocarbons, be made up of closed rings of carbon atoms. Ring structures are found in hydrocarbons, sometimes with the presence of double bonds. The benzene ring is present in many biological molecules including some amino acids and most steroids. Benzene is a natural component of crude oil and has been classified as a carcinogen. [3]

Chapter 2: Simulations and Methods

2.1 Density Functional Theory (DFT)

Density-functional theory (DFT) is a successful theory to calculate the electronic structure of atoms, molecules, and solids. Its goal is the quantitative understanding of material properties from the fundamental laws of quantum mechanics. DFT calculations are performed, in this work, with GPAW[31]. It is an efficient program package for electronic structure calculations. It is based on DFT implemented within the projector augmented wave (PAW).

Traditional electronic structure methods attempt to find approximate solutions to the Schrödinger equation of N interacting electrons moving in an external, electrostatic potential. But it is quite difficult to achieve something like this, even for small systems, and for larger numbers of N the description is not allowed. At the same time it is a problem that is not at all familiar, so that there are not many research projects, because the resulting wave functions are complex objects.

A different approach is taken in density-functional theory where, instead of the many-body wave function, the electron density is used as the fundamental variable. Since the density is a function of only three spatial coordinates (rather than the 3N coordinates of the wave function), density-functional theory is computationally possible even for large systems. [8]

DFT calculation provides more accurate result but this calculation is applicable for small system and based on quantum methods. On the other hand, empirical interatomic potentials calculations are more significant for big systems and based on classical mechanics. And this is how molecular dynamics come into play.

2.2 Molecular Dynamics

The ease with which computers can be used has allowed the current generation of scientists to meet the demands of engineers for solutions to complex problems and to push the boundaries to what is technologically possible. Two distinct sciences have evolved along with the development of the computer. One is computer science which examines the logic, design and control of computers, the representation and organization of data structures, the design of programming languages and operating systems, etc. The other is computational science - the science of computation rather than computers. It is the older of the two, established much earlier under the name of "numerical methods". This examines the various means by which functions can be approximated, or differentiated and integrated. It deals with optimization techniques, finding the roots in equations, solving systems of linear, ordinary and partial differential equations - in fact, any analytical methods face a "bunch" of problems, numerical methods try to give an answer to them.

Computational science forms the mathematical backbone of computational physics. A computational physicist tries to reach approximate solutions to problems that are otherwise difficult to obtain. For a system with a stable state a computational solution would normally be a graph representing the relationship between two or more parameters. For a dynamic, time-varying system, computations can trace its behavior over time and space, in effect recreating the system itself. Such a recreation is usually called a 'computer simulation', and if the simulation is necessarily complete it is referred to as a 'computer experiment'.

Molecular dynamics (MD) is a computer simulation method for analyzing the physical movements of atoms and molecules. The atoms and molecules are allowed to interact for a fixed period of time, giving a view of the dynamic "evolution" of the system, so the system physical properties are monitored. Those properties are either macroscopic system properties, [V (volume), P (pressure), T (temperature), N (number of particles)], or microscopic system properties, [v_i (velocities), r_i (positions)].[16] In the most common version, the trajectories of atoms and molecules are determined by numerically solving Newton's equations of motion for a system of interacting particles, where forces between the particles and their potential energies are often calculated using interatomic potentials or molecular mechanics force fields. [10]

This research includes NVE and NVT simulations. The micro canonical ensemble NVE signifies a system where the number of atoms, the system volume and the total energy (the sum of potential and kinetic energy) are kept constant. The equations of motion are solved and the positions and velocities are updated every subsequent time step.

The canonical ensemble NVT contains all possible states in thermal equilibrium with a heat bath. The system remains in the absolute temperature T but may exchange energy with the heat bath. Three parameters of the system are fixed throughout the simulation: the absolute temperature (T), the number of atoms (N), and the volume (V). [16]

In this work we used the LAMMPS software. It stands for Large-scale Atomic/Molecular Massively Parallel Simulator. It is a classical molecular dynamics simulation code with a focus on materials modeling. It was designed to run efficiently on parallel computers. It was developed originally at Sandia National Laboratories, a US Department of Energy facility. [11] [20]

Before we start with the simulations, we need to build the structures and for this it is necessary to define the positions of the atoms. The atomic simulation environment (ASE)[32] is a software package written in the Python programming language with the aim of setting up, visualizing, steering, and analyzing atomistic simulations. In ASE, tasks are fully scripted in Python. The powerful syntax of Python combined with the NumPy array library make it possible to perform very complex simulation tasks.[12] In

this work we used ASE to make structures such as diamond and graphene nanoribbons.

Depending on whether the system is 2 or 3 dimensions, the positions are determined by a series of vectors containing the x, y, and z coordinates. In the case of LAMMPS, the initial positions of the atoms can be user defined, which involves a data file containing the position vector of each atom in the system. When setting the initial positions, it must be taken into account that they correspond to the desired minimized structure, else the simulation will be inaccurate. For this reason we first start to minimize the structures before starting the simulation.

Minimum energy configuration corresponds to the stable state of the system. Stable states of molecular systems correspond to global and local minima on their potential energy surface. Starting from a non-equilibrium molecular geometry, energy minimization employs the mathematical procedure of optimization to move atoms so as to reduce the net forces on the atoms until they become negligible. Energy minimization is a numerical procedure for finding a minimum on the potential energy surface starting from a higher energy initial structure. During energy minimization, the geometry is changed in a stepwise way so that the energy is reduced. After a number of steps, a minimum on the potential energy surface is reached.

2.3 Bond Order Potential

In this work we chose to use classical empirical potentials as they can be used to model much larger systems, with varying temperature and for longer time, allowing, for example, the study of point, line and planar defects. However, one of the biggest drawbacks of classical simulations is that results are only as good as the force-field used to obtain them. Because of that, the two main problems related to the use of classical-mechanics simulations are the transferability and the version-control of the originally developed potentials. Transferability is the ability of a potential to produce reliable results when simulating conditions other than those used in the fitting process. Originally, empirical dynamics were created for some specific materials in order to calculate properties (e.g. mechanical properties) at some specified temperature. Therefore it is important to test if the same potential performs for other crystal structures for a range of temperatures as it is difficult to fit perfectly transferable potentials. The second major worry related to the use of classical potentials is the possibility that the potential form actually implemented in the used code is not exactly identical to the form initially distributed by the developers. File formats change between codes and errors can be made during transfer or the files can get destroyed. [27]

Bond order potential is a class of empirical (analytical) interatomic potentials which is used in molecular dynamics and molecular statics simulations. Examples include the Tersoff potential and the Brenner potential. [6]

General form for many body potential:

$$E = \sum_{i<j} V_2(r_{ij}) + \sum_{i<j<k} V_3(r_{ij}, r_{jk}, r_{ik}) + \ldots$$

The first term is a two-body potential, which can include repulsive and attractive terms. The second term is a three-body potential, which prevents the automatic close packing of the particles in the system. Powerful approach for modeling any type of bonding. But it can be improved by including explicit information about the surroundings of each atom.

Tersoff proposed a new potential form:

- Multiply the two-body term by a bond-order term, bij, which is decided by the local environment (it is a many-body term).
- Bij weighs the bond strength and is a monotonically decreasing function of the number of competing bonds, the strength of the competing bonds and the cosines of the angles with competing bonds.

$$E = \sum_i \sum_{i<j} \left[V_R(r_{ij}) + \overline{b_{ij}} V_A(r_{ij}) \right]$$

$$\overline{b_{ij}} = \frac{1}{2}\left(b_{ij} + b_{ji}\right)$$

$$b_{ij} = \left(1 + \beta^n \cdot \left(\sum_{k \neq i,j} f_c(r_{ik}) g(\theta_{kij}) e^{\lambda_3^3 (r_{ij} - r_{ik})^3} \right)^n \right)^{\frac{-1}{2n}}$$

$$g(\theta_{kij}) = 1 + \frac{c^2}{d^2} - \frac{c^2}{d^2 + (h - \cos\theta)^2}$$

The original Tersoff potential was designed for Silicon and Carbon and was able to describe single, double, and triple bond configurations, but it was not able to describe radicals and conjugate versus non-conjugate structures. This led to the development of the REBO potential (Reactive Empirical Bond Order potential), which is a Tersoff-like potential, developed by Brenner.[9]

Second generation of REBO potential: The first generation REBO was improved by modifying the angular term and adding a torsion term.

Modified angular term: New function, new fit method, flexible in various bond angles during the chemical reaction.

Added the torsion term: Provides the rotation barrier for double bond and conjugate bond. [7]

The main difference between the two potentials is that REBO can calculate bond energies for atoms of different coordinations. For example, while the Tersoff potential can describe the covalent bonding in a system of carbon atoms only, the REBO

potential can handle a hydrocarbon system. This makes REBO very useful in describing a system of multiple species.

2.4 Radial Distribution Function (RDF)

One way to characterize a structure is by using the Radial distribution function, (or pair correlation function). RDF g(r) in a system of particles (atoms, molecules, colloids, etc.), describes how density varies as a function of distance from a reference particle.

$$\rho g(r) = \frac{1}{N} \left\langle \sum_{i=1}^{N} \sum_{\substack{j=1 \\ (j \neq i)}}^{N} \delta(r - r_{ij}) \right\rangle$$

In other words, the radial distribution function (RDF) defines the probability of finding a particle at distance r from another tagged particle. It shows a set of peaks at positions that correspond to shells around a given atom. The function carries information on the structure of the system. (see Figure 2.4.1) [5]

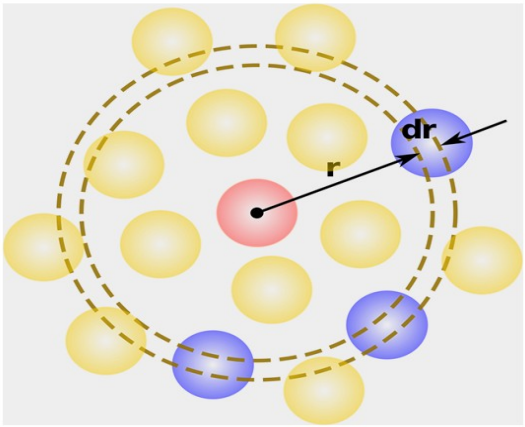

Figure 2.4.1 [5]: calculation of g(r)

2.5 Vibrational Spectra & Fast Fourier Transform

Vibrational modes

Molecules vibrate. A single molecule can vibrate in various ways and each of these different motions is called a vibration "mode". Degree of freedom is the number of variables required to describe the motion of a particle completely. For an atom moving in 3-dimensional space, three coordinates are adequate so its degree of freedom is three. Its motion is purely translational. If we have a molecule made of N atoms (or ions), the degree of freedom becomes 3N, because each atom has 3 degrees of freedom. Additionally, since these atoms are bonded together, all motions are not translational: some become rotational, some others vibration. For non-linear molecules, all rotational motions can be defined in terms of rotations around 3 axes, the rotational degree of freedom is 3 and the remaining 3N-6 degrees of freedom

constitute vibrational motion. For a linear molecule however, rotation around its own axis is no rotation because it leaves the molecule unchanged. So there are only 2 rotational degrees of freedom for any linear molecule leaving 3N-5 degrees of freedom for vibration.

The degrees of vibrational modes for linear molecules can be calculated using the formula: 3N−5.The degrees of freedom for nonlinear molecules can be calculated using the formula: 3N−6

A normal mode of a dynamical system is a pattern of motion in which all parts of the system move sinusoidally with the same frequency and with a fixed phase relation. The free motion described by the normal modes takes place at fixed frequencies. These fixed frequencies of the normal modes of a system are known as its natural frequencies or resonant frequencies. A physical object, such as a molecule, has a set of normal modes and their natural frequencies that depend on its structure, materials and boundary conditions. [24] The local vibrational modes are the true equivalent of the normal vibrational modes.

A molecular vibration is a periodic motion of the atoms of a molecule relative to each other, such that the center of mass of the molecule remains unchanged.[14] Within the CH_2 group, commonly found in organic compounds, the two low mass hydrogens can vibrate in six different ways which can be grouped as 3 pairs of modes: 1. symmetric and asymmetric stretching, 2. scissoring, and rocking, 3. wagging and twisting. These are shown in Figure 4 [13]:

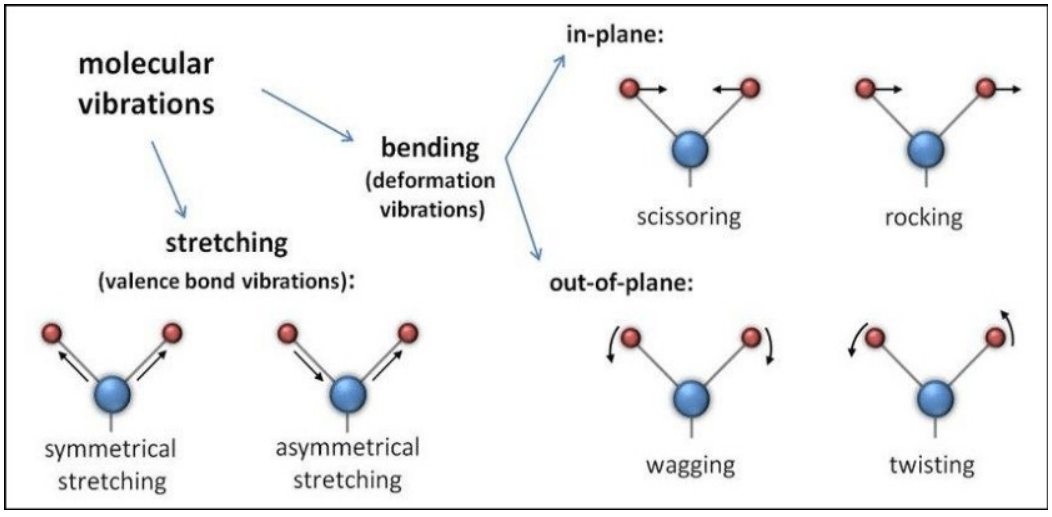

Figure 2.5.1 [13]: Visualization of all different molecular vibrations

Stretching and Bending modes

A stretching vibration changes the bond length. There are two types of stretching vibrations. In symmetric stretching, two or more bonds vibrate in and out together. In asymmetric stretching, some bonds are getting shorter at the same time as others are getting longer, resulting in a change in the dipole moment of the molecule. So, asymmetric stretching appears at a higher wavenumber and absorbs or needs more

energy than symmetric stretching. Bending vibrations are characterized by a change in the angle between two bonds and are of four types: scissoring, rocking, wagging, and twisting. (See Figure 2.5.1)

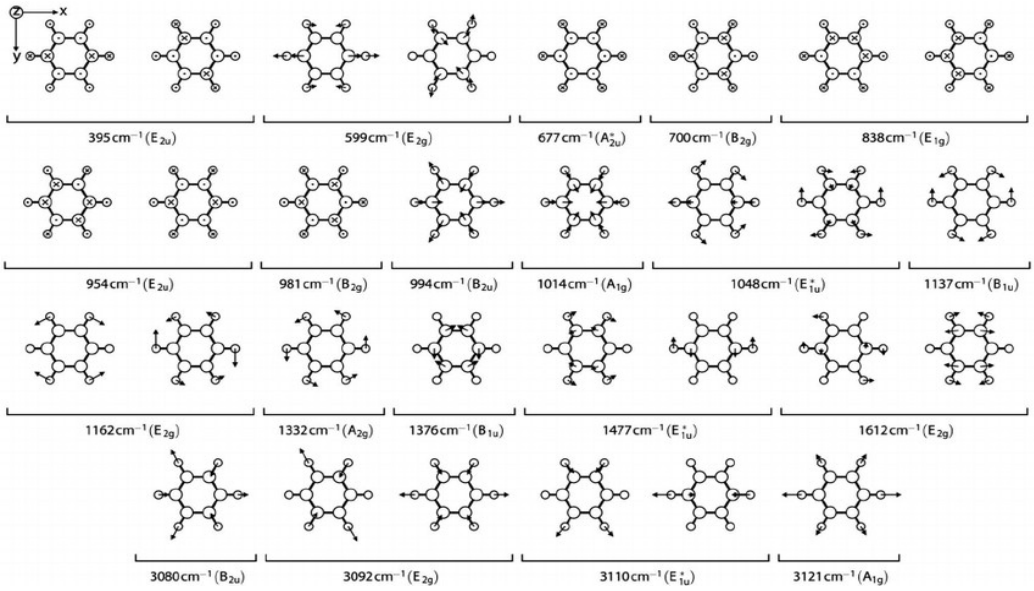

Figure 2.5.2: Graphic representation of the normal modes of benzene and their symmetry classification. C (H) atoms are shown as large (small) circles. Out-of-plane modes are shown in such a way that atoms bearing dots (crosses) are displaced forwards (backwards). For the in-plane modes arrows to scale for each mode indicate atomic displacements in the paper plane. Infrared-active modes are labeled with an asterisk. [21]

Fast Fourier Transform (FFT)

A given function or signal can be converted between the time and frequency domains with a pair of mathematical operators called transforms. An example is the Fourier transform, which converts a time function into a complex valued sum or integral of sine waves of different frequencies, with amplitudes and phases, each of which represents a frequency component. The "spectrum" of frequency components is the frequency-domain representation of the signal. [25]

The "Fast Fourier Transform" (FFT) is an important measurement method in the science of audio, acoustics measurement and electromagnetic signal processing. It converts a signal into individual spectral components and thereby provides frequency information about the signal. FFTs are used for fault analysis, quality control, and condition monitoring of machines or systems. Strictly speaking, the FFT is an optimized algorithm for the implementation of the "Discrete Fourier Transformation" (DFT). A signal is sampled over a period of time and divided into its frequency components. These components are single sinusoidal oscillations at distinct frequencies each with their own amplitude and phase.

From [15] we see that two parameters are relevant:

- The sampling rate or sampling frequency Δt of the measuring system: if Δt is measured in seconds, then the sampling rate is the number of samples recorded per second.
- The selected number of samples N: This is always an integer power to the base 2 in the FFT (e.g., $N = 2^{11} = 2048$ samples)

From the two basic parameters Δt and N, further parameters of the measurement can be determined.

- Nyquist frequency f_c: This value indicates the theoretical maximum frequency that can be determined by the FFT.

$$f_c = \frac{1}{(2 * \Delta t)}$$

- Frequency resolution Δf. The frequency resolution indicates the frequency spacing between two measurement results.

$$\Delta f = \frac{1}{(N * \Delta t)}$$

A small N results in fast measurement repetitions with a coarse frequency resolution. A large N results in slower measuring repetitions with fine frequency resolution. [15]

Below we listed the parameters we used in this project for FFT calculations:

1. Number of points we kept: 2048
2. Sampling rate Δt: 10^{-15} seconds
3. Frequency resolution Δf: 16,3 cm^{-1} or 0,488 THz
4. Steps in MD simulations (LAMMPS): 100000
5. Time unit dt (LAMMPS): 0,0001ps or 0,1fs
6. Every 10 steps we store the positions and velocities in data file(LAMMPS)

Chapter 3: Results and Discussion

3.1 Calculation of diamond lattice constant with DFT

In the Figure below is the Diamond structure of 8000 atoms we made with ASE.

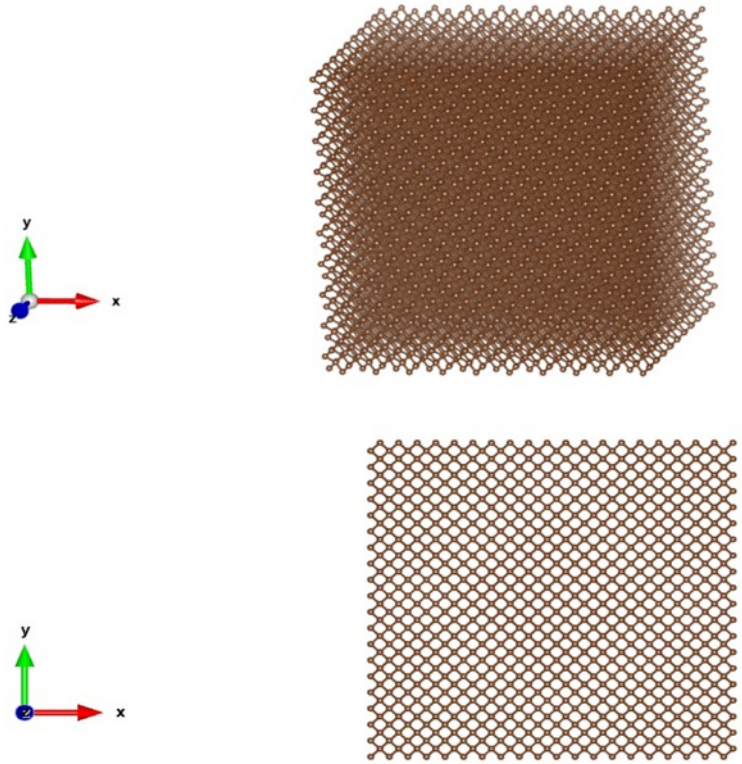

Figure 3.1.1: Diamond Structure of 8000 atoms

We will start with the analysis of the results of the lattice constant calculation of Diamond by using the Density Functional Theory (DFT) method, with the software GPAW. First we measured the energy of a unit cell of the system in Figure 3.1.1 and after that, by changing the lattice constant manually, we get the energy for each value and plot the energy vs lattice constant graph. Then by fitting a second degree polynomial we calculate the minimum value of the graph and the material's lattice constant was calculated 3.54Å. For the graphs below we used two softwares, SciDAVis and Excel, and for the structure visualization VESTA.

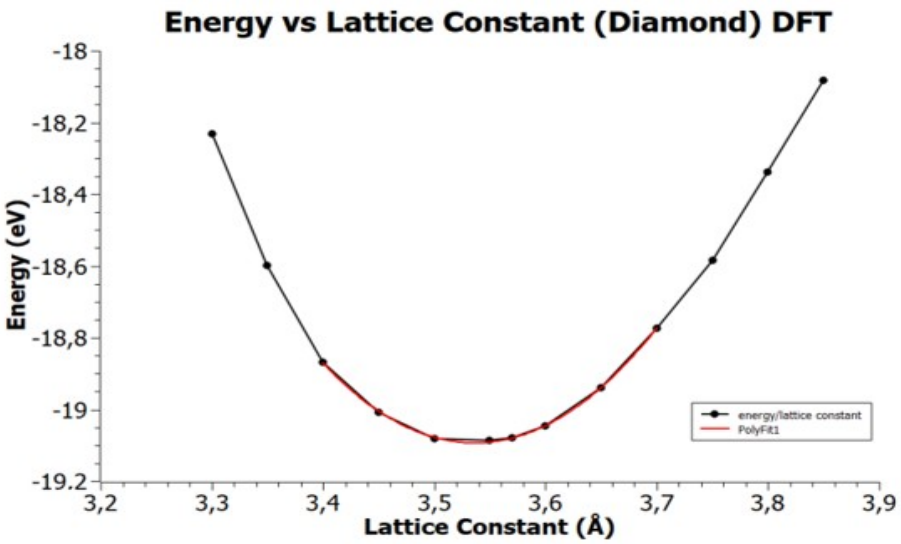

Figure 3.1.2: Energy vs Lattice constant Graph for Diamond structure with DFT

3.2 Calculation of diamond lattice constant with empirical potentials and cg algorithm

For the diamond structure of 8000 atoms the change of the lattice constant is done with the command "lattice" of LAMMPS. From all the values obtained, we plot the energy/lattice constant graph. Then, with a second degree polynomial we calculated the minimum of the curve and the theoretical lattice constant. First we used the Brenner potential and then the Tersoff potential. Below we show in black the curve of the theoretical points, and in red the approximation of the curve near the minimum with a second degree polynomial ($y = a\,x^2 + bx + c$).

- Brenner

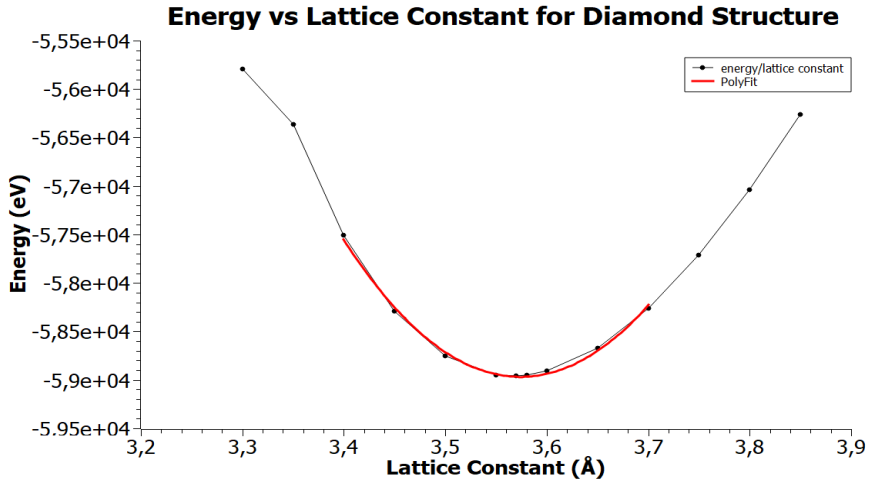

Figure 3.2.1: Energy vs Lattice constant Graph for Diamond structure with the Brenner Potential

Results Log

[12/5/2022 9:53 πμ Plot: "Graph1"]
Polynomial fit of dataset: Table2_-55.928, using function: a0+a1*x+a2*x^2
Y standard errors: Unknown
From x = 3,4 to x = 3,7
a0 = 538.606,231282871 +/- 18.436,6415137714
a1 = -334.388,37304843 +/- 10.397,9600876109
a2 = 46.778,8225611857 +/- 1.465,41582571795

Chi^2 = 8.494,59294024219
R^2 = 0,995514627157991

Therefore from the second degree polynomial:

$$y = 46.778{,}82\,x^2 - 334.388{,}37\,x + 538.606{,}23$$

We calculate the minimum from:

$$\frac{dy}{dx} = 2ax + b = 0 \rightarrow x = \frac{-b}{2a} \rightarrow x = \frac{-(-334.388{,}37)}{2(46.778{,}82)} = 3{,}5741428493 \ \ Å$$

$$a = 3{,}57\,Å$$

The experimental value is: a = 3,57Å

Comparing the theoretical with the experimental value:

$$\%\ percentage\ difference = \frac{(3{,}57\ \ Å - 3{,}57\ \ Å)}{3{,}57\,Å} \simeq 0{,}00\,\%$$

Therefore from the second degree polynomial we calculated that the lattice constant is 3,57Å and the experimental value is also 3,57Å. By comparing the theoretical with the experimental value we have a percentage difference of 0,0 % .

- Tersoff

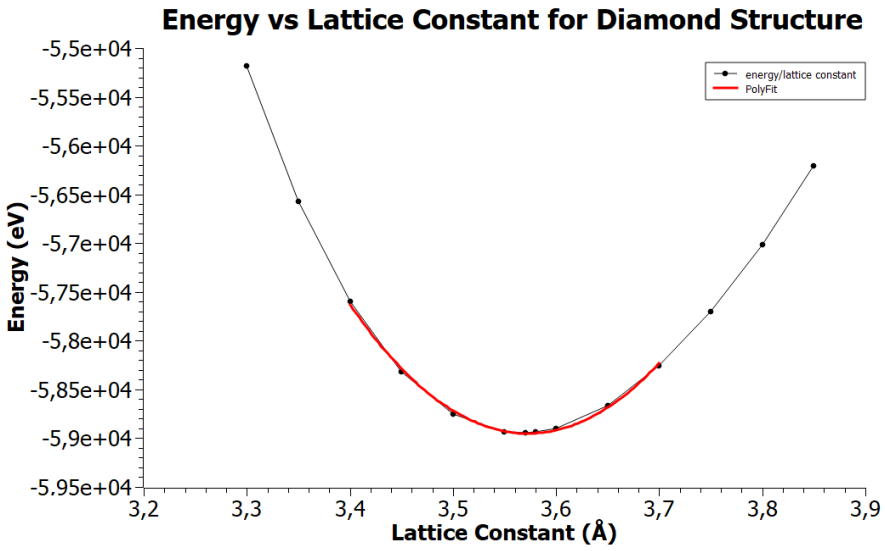

Figure 3.2.2: Energy vs Lattice constant Graph for Diamond structure with the Tersoff Potential

As in with the Brenner potential we calculated that the lattice constant is 3,57Å. So we have again a percentage difference of 0.0%.

Note: In the graphs below we have g(r) in a.u, for arbitrary units, in the y axes and r, for distance in Angstrom, in the x axes.

The last way to calculate the constant is with energy minimization with conjugate gradient (cg) algorithm with the Brenner Potential, from LAMMPS. After the minimization we use the Radial distribution function, so that we don't have to measure all the distances manually as the graph shows us the distance r of the first neighbors from the first peak.

For diamond cubic structures the lattice constant is calculated from: $d_{NN} = (a * 4)/\sqrt{3}$, where d_{NN} is the distance of first neighbors.

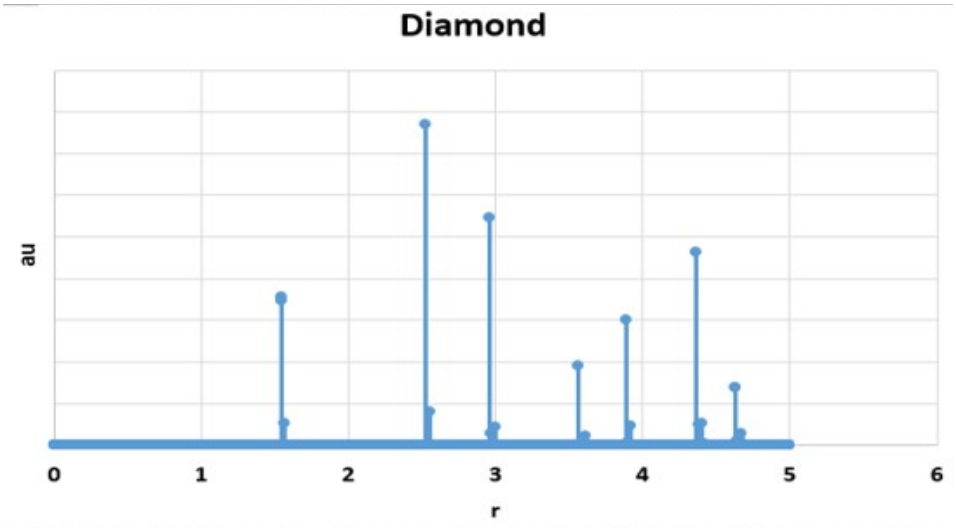

Figure 3.2.3: RDF Graph for Diamond structure with Conjugate Gradient (cg) algorithm

In Table 1 are the theoretical results, of each method, for the lattice constants of Diamond.

Theoretical Values				
Table 1	**DFT**	**Brenner**	**Tersoff**	**cg algorithm (with Brenner)**
Diamond	3,54Å	3,57Å	3,57Å	3,56Å

3.3 Calculation of graphene lattice constant with DFT

Similarly we worked for the graphene structure. We started by creating fully periodic perfect graphene lattice with 400 atoms (Figure 3.3.1).

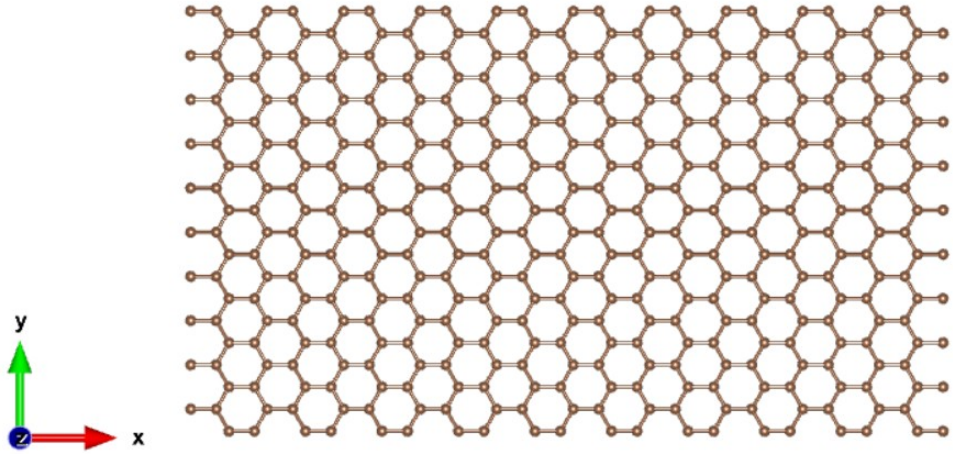

Figure 3.3.1: Graphene structure of 400 atoms

After that we used GPAW to calculate the lattice constant of Graphene with DFT, in the same way we did for Diamond bevor. The minimum value of the graph and the material's lattice constant was calculated 2.47Å

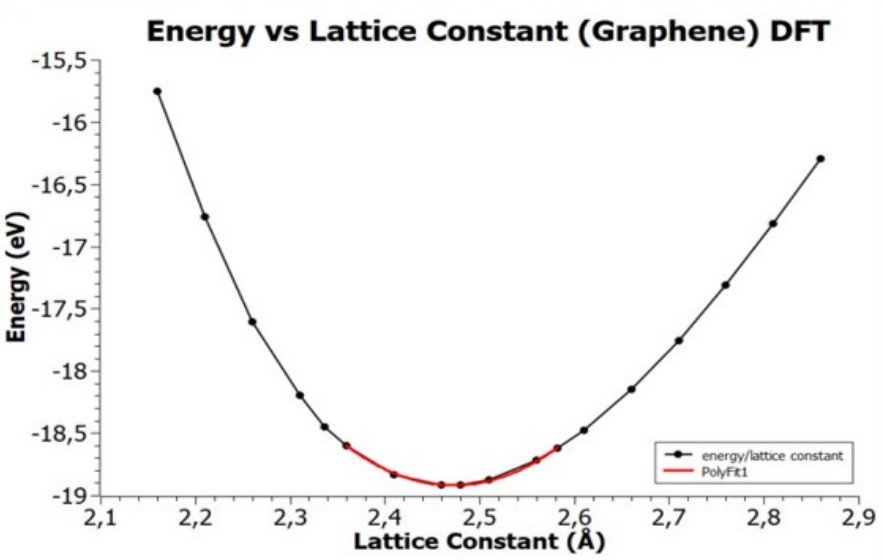

Figure 3.3.2: Energy vs Lattice constant Graph for Graphene structure with DFT

3.4 Calculation of graphene lattice constant with empirical pot entials and cg algorithm

We started by measuring the energy of the graphene structure of Figure 3.4.1. Then we changed the xyz coordinates and the dimensions of the "box" (with the help of a program written in Fortarn 95), to change the lattice constant and measure the energy again. With VESTA we visualize the structure resulting from the change and measure with maximum accuracy the lattice constant. From all the values obtained, we plot the energy/lattice constant graph. Then, with a second degree polynomial we calculated the minimum of the curve and the theoretical lattice constant.

- Brenner

With the software of VESTA we see the graphene structure and calculate the lattice constant by measuring the appropriate distances.

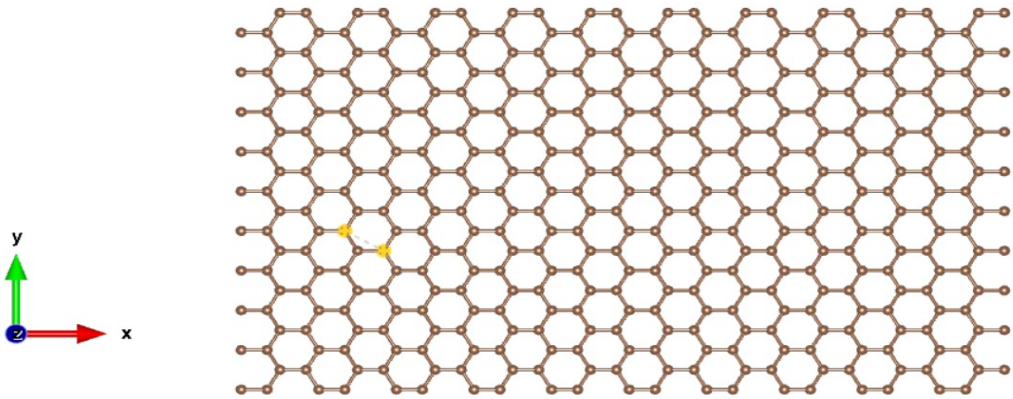

Figure 3.4.1: Graphene structure of 400 atoms

```
1(C166-C128) =  2.45949(0) Å
 166    C166  C  5.68000  9.83776  0.00000 ( 0,  0,  0)+ x, y, z
 128    C128  C  7.81000  8.60804  0.00000 ( 0,  0,  0)+ x, y, z
```

Figure 3.4.2: VESTA results of measuring the lengths between the two yellow points of Figure 3.4.1

We continue with the same procedure with other lattice constants. Below we show in black the curve of the theoretical points, and in red the approximation of the curve near the minimum with a second degree polynomial (y = a x2+ bx + c).

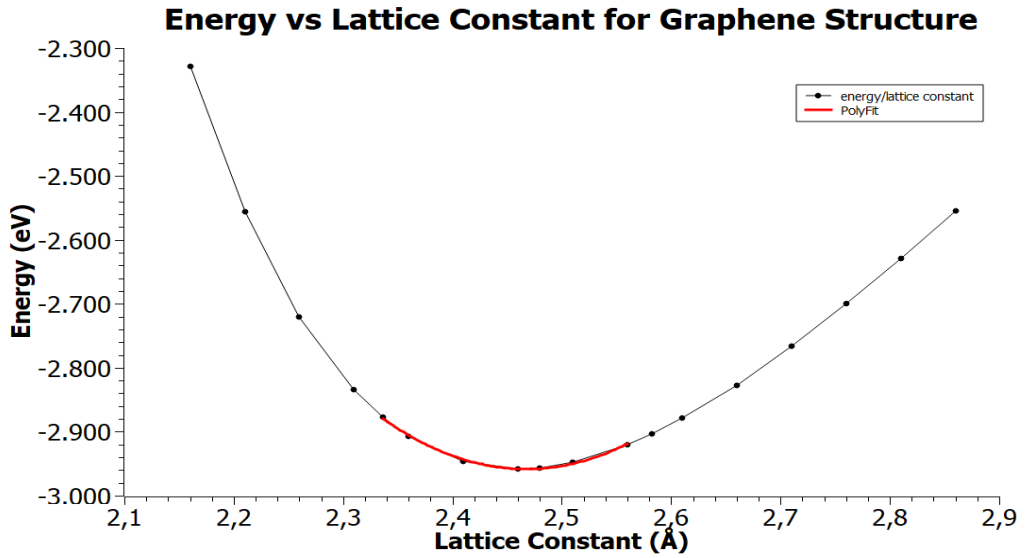

Figure 3.4.3: Energy vs Lattice constant Graph for Graphene structure with the Brenner Potential

Therefore from the second degree polynomial: $a = 2{,}47\,Å$

The experimental value for graphene is 2,46Å.

Comparing the theoretical with the experimental value:

$$\%\ percentage\ difference = \frac{(2{,}46\ Å - 2{,}47\,Å)}{2{,}46\,Å} \simeq 0{,}4\ \%$$

- Tersoff

We repeat the same steps as before so that we can plot the "Energy vs lattice constant" graph.

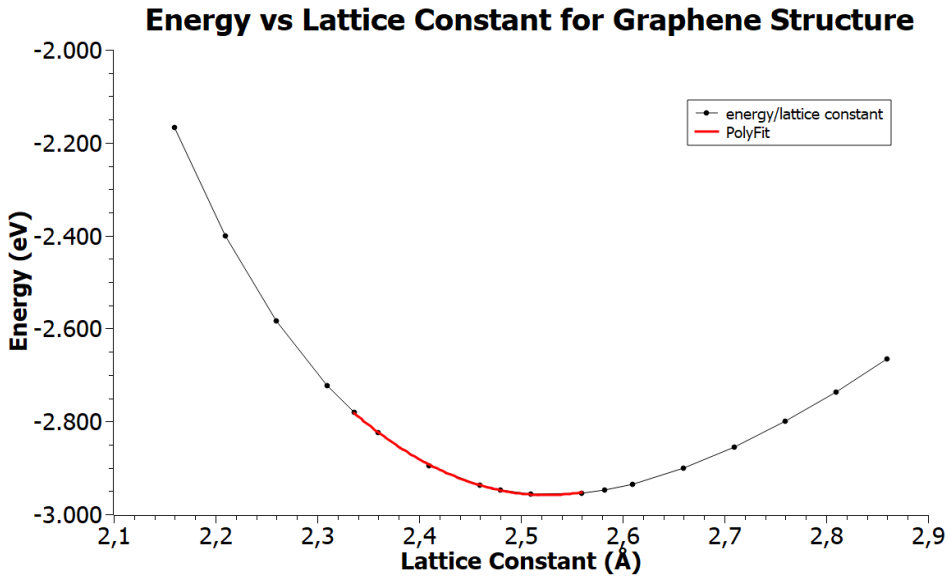

Figure 3.4.4: Energy vs Lattice constant Graph for Graphene structure with the Tersoff Potential

Therefore from the second degree polynomial we have $a = 2{,}53\ \text{Å}$

Comparing the theoretical with the experimental value:

$$\%\ percentage\ difference = \frac{(2{,}46\ \text{Å} - 2{,}53\ \text{Å})}{2{,}46\,\text{Å}} \simeq 2{,}85\%$$

For the graphene structure we observe greater accuracy with the Brenner Potential (percentage difference of 0.40%), while in the Tersoff Potential we have a percentage difference of 2.85%. In the diamond structure the experimental result agrees exactly with the theoretical value for both Potentials.

Next we calculate the lattice constant with the cg algorithm, as we did for the Diamond structure. But we mention here that for honeycomb structures the lattice constant is calculated from: $d_{NN} = a / \sqrt{3}$

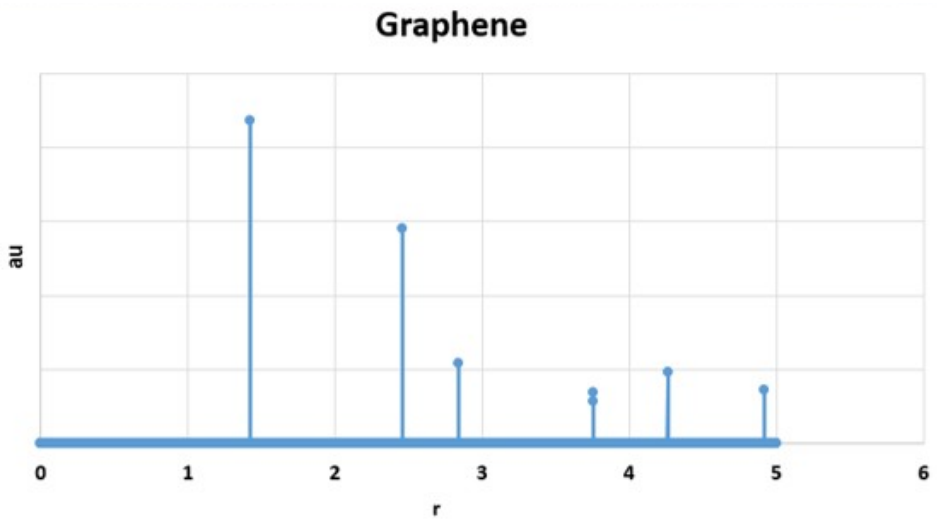

Figure 3.4.5: RDF Graph for Graphene structure with Conjugate Gradient (cg) algorithm

In Table 2 are the theoretical results, of each method, for the lattice constants of Graphene.

	Theoretical Values			
Table 2	**DFT**	**Brenner**	**Tersoff**	**cg algorithm eith Brenner**
Graphene	2,47Å	2,47Å	2,53Å	2,46Å

3.5 NVE Simulation for 10K and 300K

Note: For the graphs below we used Excel.

After applying NVE simulation first at 10K (blue) and then at 300K (orange), we plot the RDF graph for Graphene and Diamond structure as we can see below. In the

graphs, in the y axes we have g(r) in a.u, for arbitrary units, and r, for distance in Angstrom, in the x axes.

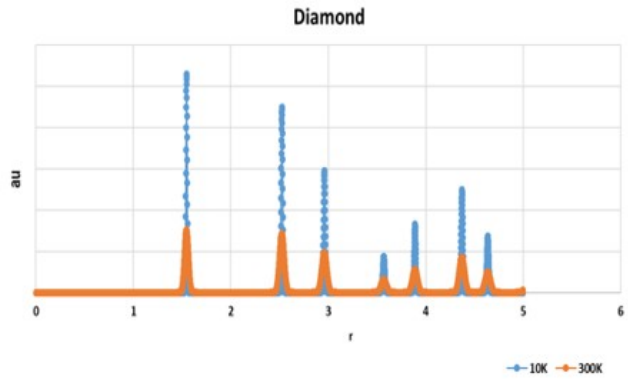

Figure 3.5.1: RDF Graphs for Diamond structure with NVE

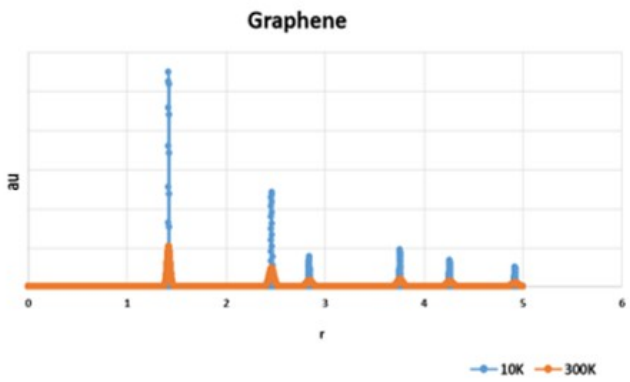

Figure 3.5.2: RDF Graphs for Graphene structure with NVE

By zooming in on the first peak we can see that the position of the peak (r value) remains the same at both temperatures, but at 300K the width of the curve has increased. This is explained by the fact that with an increase in temperature, the particles gain kinetic energy, move faster and oscillate more. The actual average speed of the particles depends on their mass as well as the temperature – heavier particles move more slowly than lighter ones at the same temperature.

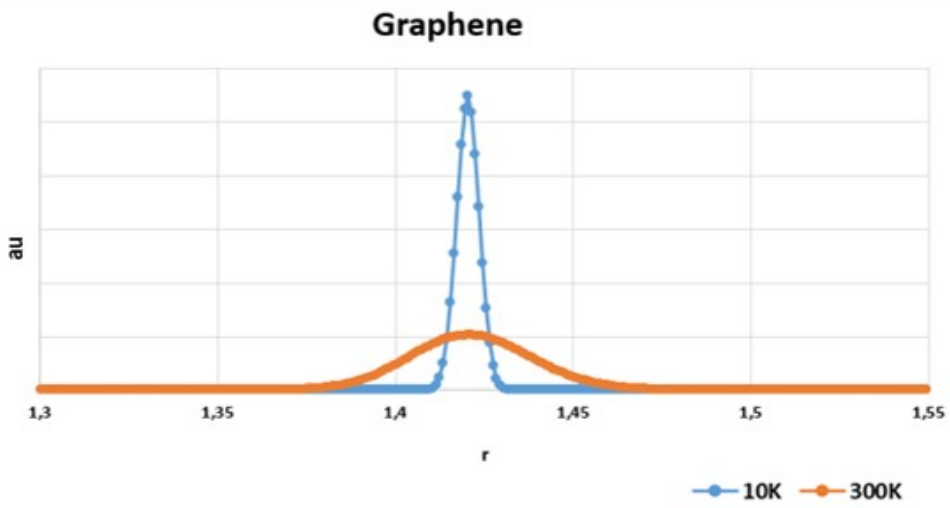

Figure 3.5.3: RDF Graphs for Graphene structure with NVE.

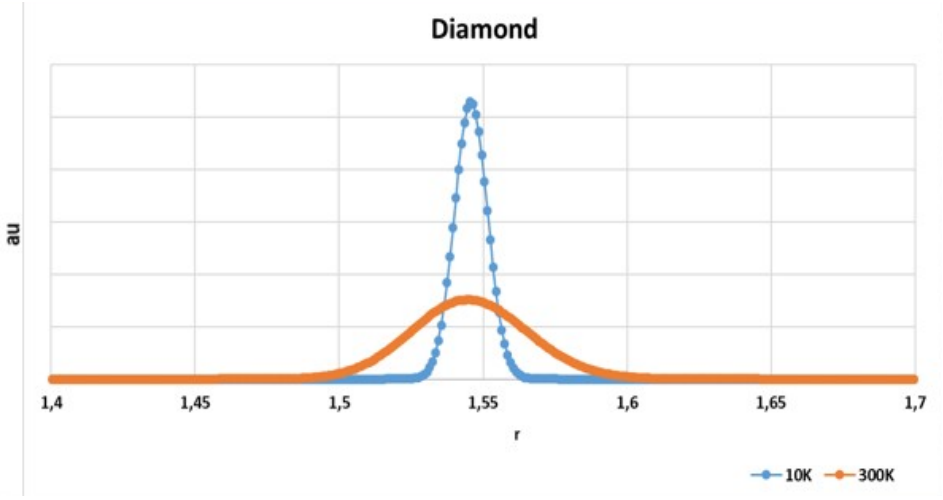

Figure 3.5.4: RDF Graphs for Diamond structure with NVE.

3.6 Small Hydrocarbon Molecules: Methane and Benzene

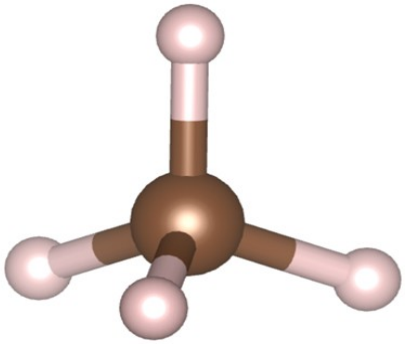

Figure 3.6.1: Methane molecule

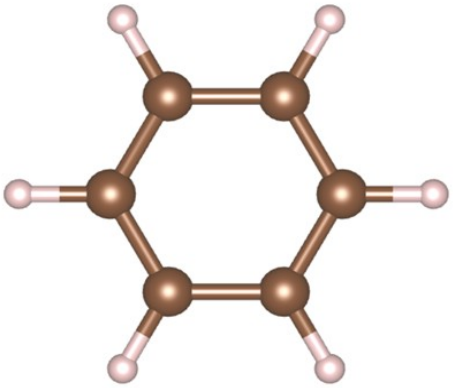

Figure 3.6.2: Benzene molecule

Next we focused on the methane and benzene molecules so we can measure bonds and angles to compare them with the experimental values and check the accuracy of LAMMPS cg minimization. As shown in Tables 3 and 4 below, there is no difference between theoretical and experimental values.

	Methane Molecule	
Table 3	**Theoretical Values**	**Experimental Values**
C-H bond	1,09 Å	1,09 Å
H-C-H angle	109,5deg	109,5deg

Table 4	Benzene Molecule Theoretical Values	Experimental Values
C-H bond	1,09 Å	1,09 Å
C-C-C angle	120 deg	120 deg
C-C bond	1,39 Å	1,39 Å

3.7 Hydrocarbon chains

Below we present three different hydrocarbon chains:

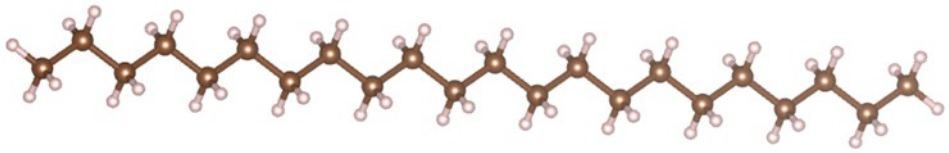

Figure 3.7.1: Hydrocarbon chain of C22H46

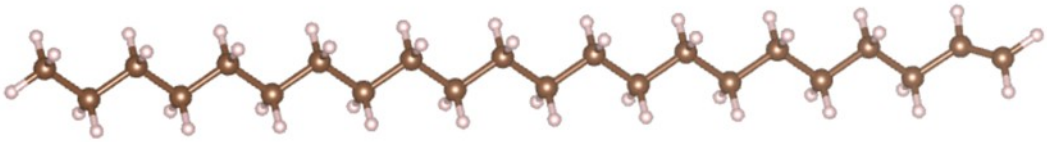

Figure 3.7.2: Hydrocarbon chain of C22H44

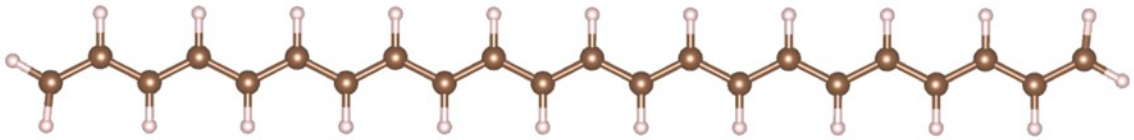

Figure 3.7.3: Hydrocarbon chain of C22H24

We focused on the structure $C_{22}H_{24}$ to compare the results with those of the article [17]. All values have been listed in Table 5. We observed that after minimization, the double and single carbon-carbon bond have the same length, which we did not expect, because at $C_{22}H_{44}$ the double bond at the right end did not change.

Table 5	Structural Values	Values from [17]
C-C single bond	1,38 Å	1,42 Å
C-C double bond	1,38 Å	1,38 Å
C-H bond	1,09Å	1,10 Å

3.8 Graphene Nanoribbons: Armchair and Zigzag

At this point in the project we present the graphene nanoribbon (GNR) structures with hydrogens on the outer carbons. We made the armchair and the zigzag structures. Below we have 1a to 1d and 2a to 2d the width 4,6,10 and 20 for each nanoribbon respectively.

Armchair Graphene Nanoribbon:

1a

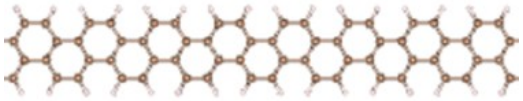

Figure 3.8.1: Armchair GNR width 4

1b

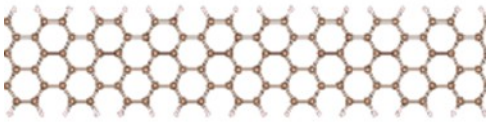

Figure 3.8.2: Armchair GNR width 6

1c

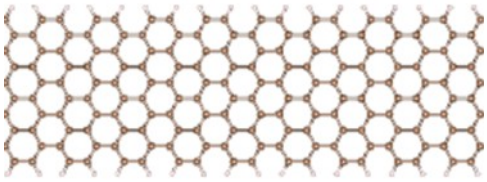

Figure 3.8.3: Armchair GNR width 10

Zigzag Graphene Nanoribon:

2a

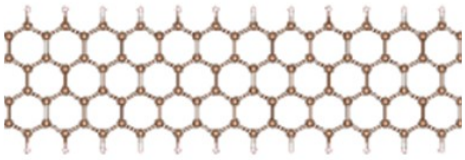

Figure 3.8.5: Zigzag GNR width 4

2b

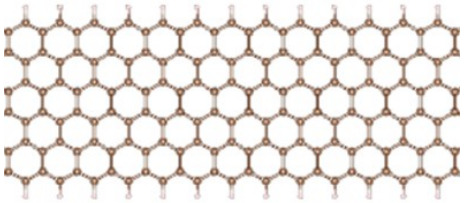

Figure 3.8.6: Zigzag GNR width 6

2c

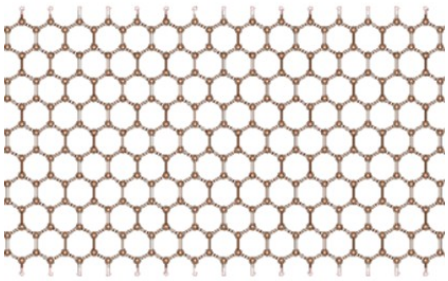

Figure 3.8.7: Zigzag GNR width 10

1d

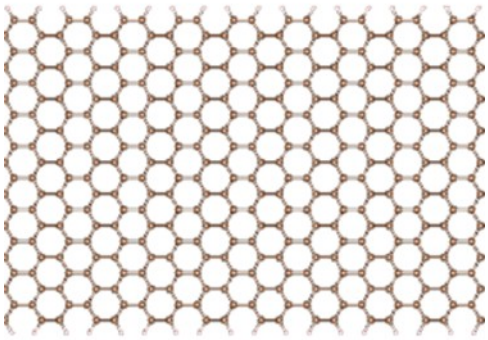

Figure 3.8.4: Armchair GNR width 20

2d

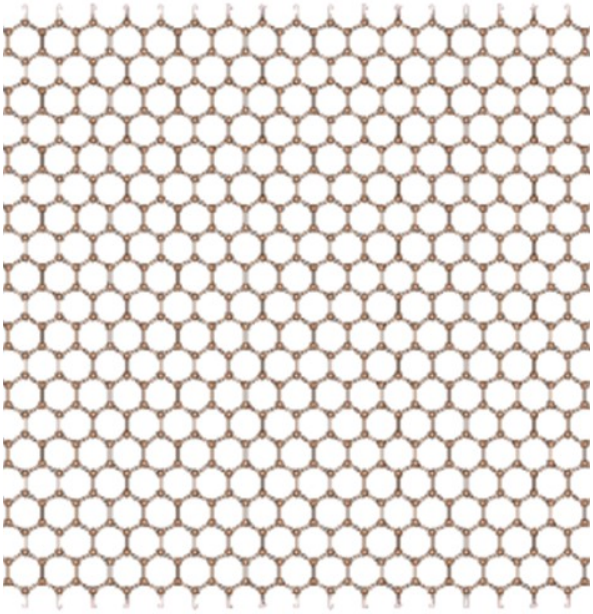

Figure 3.8.8: Zigzag GNR width 20

The aim is to observe if there is any change in the lattice constant with change in width. For this we apply the RDF graph so that we do not measure the distances by hand, as from the first peak corresponding to the first neighbor distance, we calculate the constant for each width.

Below we show two examples of the RDF graph for the armchair and zigzag graphene nanoribbon of width 4. Table 7 and 8 include the width, number of atoms and lattice constant of each nanoribbon type. In the graphs below in the y axes we have g(r) in a.u, for arbitrary units, and r, for distance in Angstrom, in the x axes.

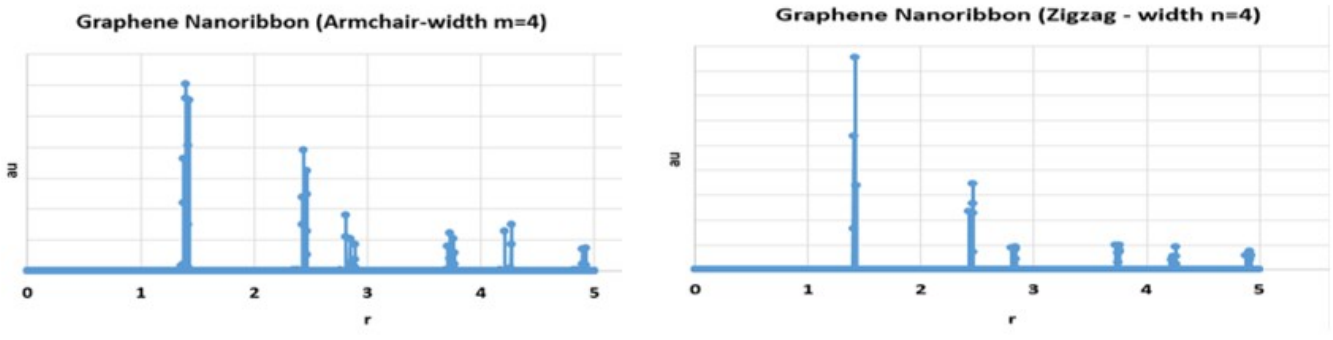

Figure 3.8.9: RDF Graph for Armchair and Zigzag Graphene Nanoribbon width 4 structure with Conjugate Gradient (cg) algorithm.

Table 7

Armchair		
Width	Number of atoms	Lattice Constant (Å)
4	480	2,4257
6	640	2,4275
10	960	2,4604
20	1760	2,4604

Table 8

Zigzag		
Width	Number of atoms	Lattice Constant (Å)
4	600	2,4604
6	840	2,4604
10	1320	2,4604
20	2520	2,4604

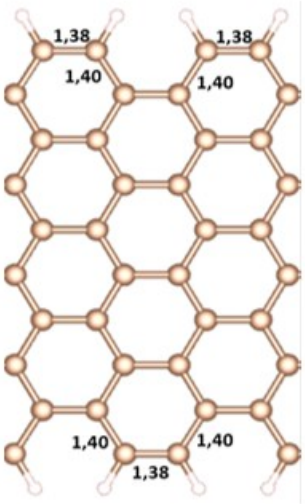

Figure 3.8.11: Armchair Graphene Nanoribbon – Width 10

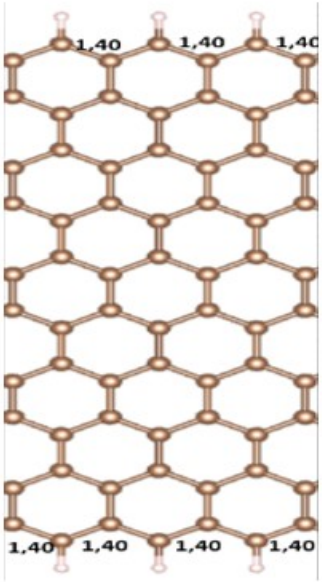

Figure 3.8.12: Zigzag Graphene Nanoribbon – Width 10

We observe in the armchair case a difference in the results, while in the zigzag structure the constant remains the same for each width. If we look in more detail at the carbon-carbon bonds in the structures, we observe something that could explain this phenomenon. As can be seen from the Figures 3.8.11 and 3.8.12, the bonds in the outer carbons are shorter. In the Armchair GNR we have values of 1.38Å and 1.40Å, while in the Zigzag GNR 1.40Å. In both cases all other C-C bonds are 1.42Å, as the experimental value.

3.9 Vibrational Spectra and Displacements of H-atoms

Vibrational Spectra

The vibrational spectra of the structures below were computed by Fast Fourier transform of the velocities (see Appendix A) computed from the trajectories generated by MD simulations using the LAMMPS package, for 100000 steps. Metal units are being used which uses picoseconds for time, Angstroms for length, Kelvin for temperature. The force field is set to the REBO potential. An NVE run is to be done with temperature rescaling to a wanted temperature of 300 or 10 K. The positions and velocities of all atoms will be written into the dump file every 10 time steps.

It's important to note that the sampling rate must be greater than the highest frequency component of the signal to ensure the sampled data accurately represents the input signal, according to the Nyquist sampling theorem.

Normal vibrational modes

We performed NVT simulation at 300K or 10K on the minimized structure for 100000 steps and stored the positions and velocities of each atom at the step in which the temperature was closer to the desired temperature of 300K or 10K. Then we used this data to perform NVE simulation to obtain the vibrational spectrum of the structure. We should mention here that equilibration was done before we got the spectrum data.

Methane: NVT simulation: T = 300.05118 K.

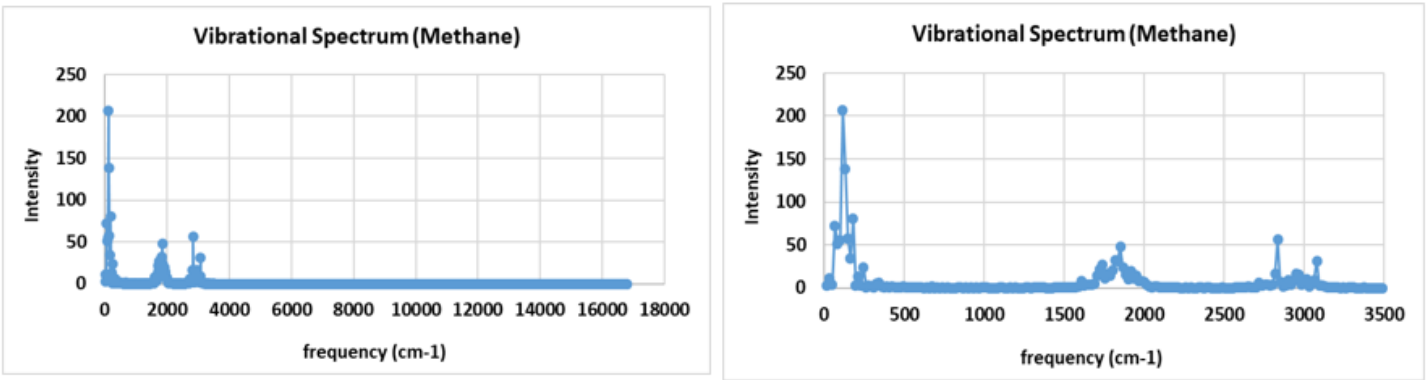

Figure 3.9.1: Vibrational spectrum of methane molecule

In methane, from Figure 3.9.1, vibrational symmetric stretch is 2835cm^{-1} ,while experimental frequency, is 2917cm^{-1}, vibrational degenerated stretching mode is 3081 cm^{-1} while for experimental frequency, it is 3019cm^{-1} (stretch), vibrational mode of degenerated deformation for experimental frequency, is 1306cm^{-1} (bend). One more degenerated deformation observed of vibrational mode is 1737cm^{-1}, while for experimental frequency, it is 1534 cm^{-1}.

Benzene: NVT simulation: T=301.75682 K.

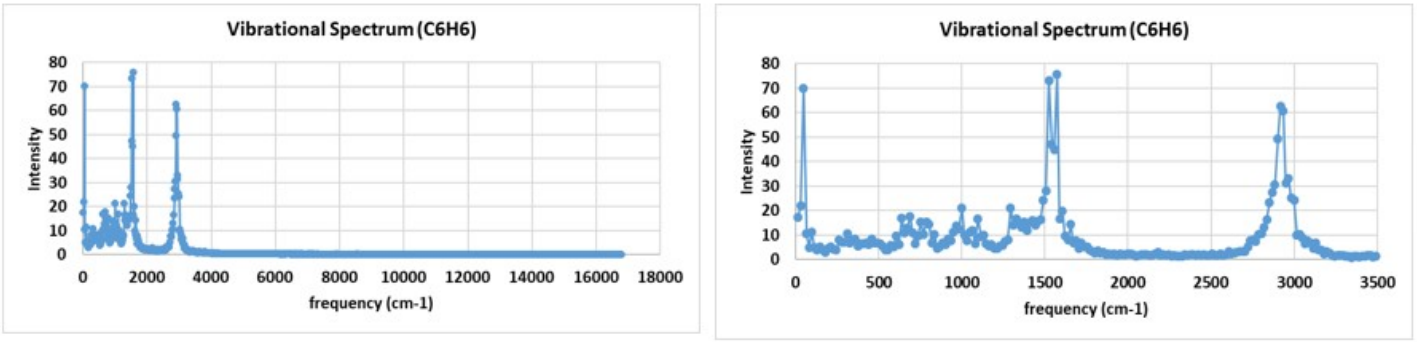

Figure 3.9.2: Vibrational spectrum of benzene molecule

The carbons in aromatic rings are unsaturated, which means hydrogens can be added to these carbons via reaction. For example, benzene, C_6H_6, can be hydrogenated to form cyclohexane, C_6H_{12}, which is not an easy reaction to perform but has been done. As a result of being unsaturated carbons, the force constant for C-H stretching in aromatic rings is higher than for saturated carbons. As a result, in general unsaturated C-H stretches fall above 3000 cm^{-1}, and saturated C-H stretches fall below 3000 cm^{-1}. This is a useful dividing line to remember for an initial examination of a spectrum. First, we have to look if there are any peaks between 2800 and 3200cm^{-1}. If there are, then these are C-H stretching peaks. Next, we look at where the peaks are in this range. If there are peaks above 3000 cm^{-1} then the carbons in the sample are unsaturated only. If all of the C-H stretches are below 3000 cm^{-1} all the carbons in the sample are saturated. If there are C-H stretches above and below 3000 cm^{-1} there are saturated and unsaturated carbons present. The 3000 cm^{-1} dividing line between the C-H stretches of unsaturated and saturated carbons has very few exceptions and is a very reliable rule of thumb.

As we read the spectrum of Figure 3.9.2 of benzene from left to right, we note there are some peaks between 2800 and 3050cm^{-1}, making these C-H stretches, with saturated and unsaturated carbons, but the main peak in this area is at 2917,19 cm^{-1}.The peaks at 1524 and 1573cm^{-1} are examples of ring mode peaks. A ring mode is a vibration that involves the stretching and contracting of the carbon-carbon bonds in an aromatic ring. These are typically sharp, but vary in number and intensity depending upon the molecule. They usually fall between 1620 and 1400cm^{-1}. The region between 1000 and 1200cm^{-1} is where aromatic ring C-H in-plane bending peaks fall. These peaks are generally medium to weak in intensity, show up in a very busy spectral region, and hence are not useful group wavenumbers.

The peaks in Figure 3.9.2, are out-of-plane C-H bends. Since aromatic rings are planar, all the hydrogens are in the plane of the molecule. When these hydrogens bend above and below the plane of the molecule they are undergoing a C-H out-of-plane bend, which is sometimes called a wag. This vibration gives rise to peaks that typically fall between 700cm^{-1} and 1000cm^{-1}. In the spectrum of benzene, this peak

usually falls at 674 cm^{-1} because the molecule is unsubstituted. In Figure 3.9.2 we see peaks between 600 and 1100cm^{-1}.

In general, the peaks between 600 and 1000 cm^{-1} are out-of-plane C-H bends. Since aromatic rings are planar, all the hydrogens are in the plane of the molecule. When these hydrogens bend above and below the plane of the molecule they are undergoing a C-H out-of-plane bend, which is sometimes called a wag. This vibration gives rise to a peak that typically falls between 1000 cm^{-1} and 700 cm^{-1} but in the spectrum of benzene, this peak falls at 674 cm^{-1} because the molecule is unsubstituted.

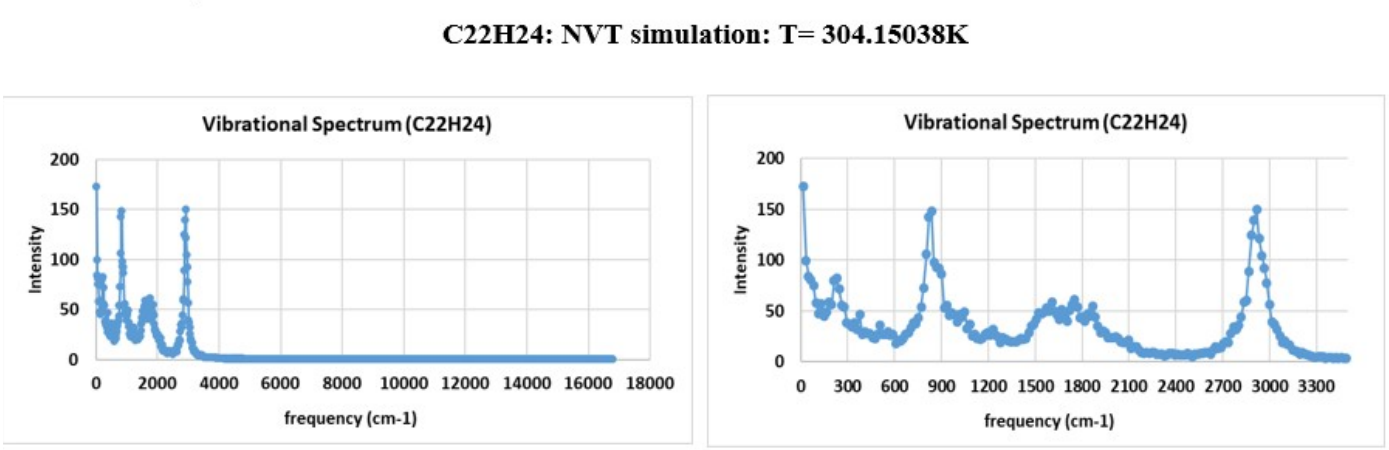

Figure 3.9.3: Vibrational spectrum of C22H24

$C_{22}H_{24}$ belongs to the category of C_nH_{n+2} and therefore we will compare the vibrational frequencies of the spectrum in Figure 3.9.3 with those of [30] for C_2H_4 (ethylene). Reading the right graph of Figure 3.9.3 from left to right we observe the first sharp peak at 835,8cm^{-1}. Similarly for ethylene there is the H-C-H in-plane rocking vibration at 835cm^{-1}. In addition, there is a peak at 885 cm^{-1} which appears in the vibrational spectrum of ethylene at 875 cm^{-1} and represents the H-C-H out-of-plane twisting vibration. We will find the C-C stretching mode of C_2H_4 at 1827cm^{-1} but in $C_{22}H_{24}$ at 1868,3cm^{-1}, which means that there is a percentage difference of 2,26%. Finally, there is a peak at 2917,2cm^{-1}, which must represent the C-H asymmetric stretching vibration, since C-H symmetric stretching is present in ethylene at higher frequencies (3210-3217cm^{-1}), which do not exist in our spectrum.

Graphene (400 atoms): NVT 300K simulation: T = 300.40552K

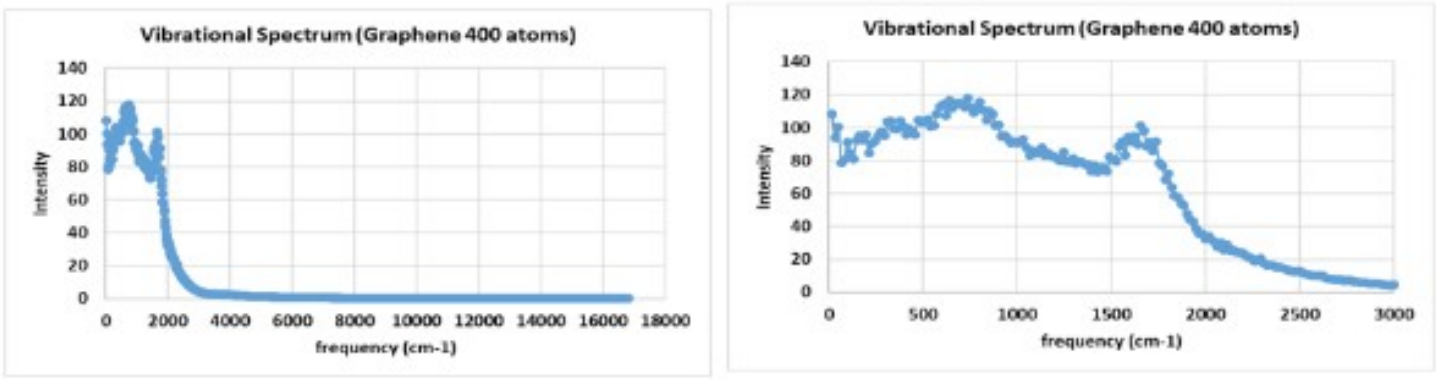

Figure 3.9.4: Vibrational spectrum of Graphene

NVT 10K simulation: T = 10.254534K

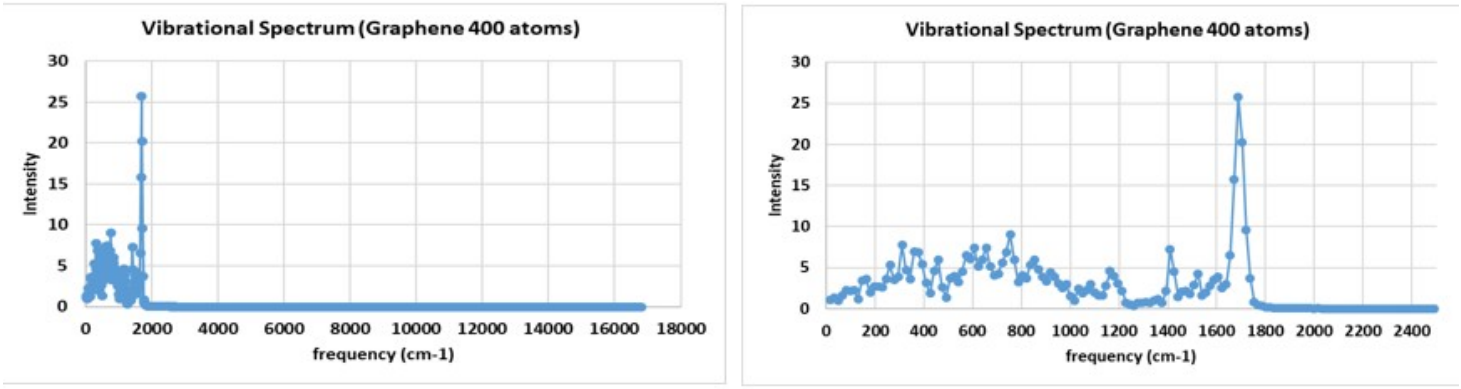

Figure 3.9.5: Vibrational spectrum of Graphene

Diamond 216 (atoms): NVT 300K simulation: T = 308.96538K

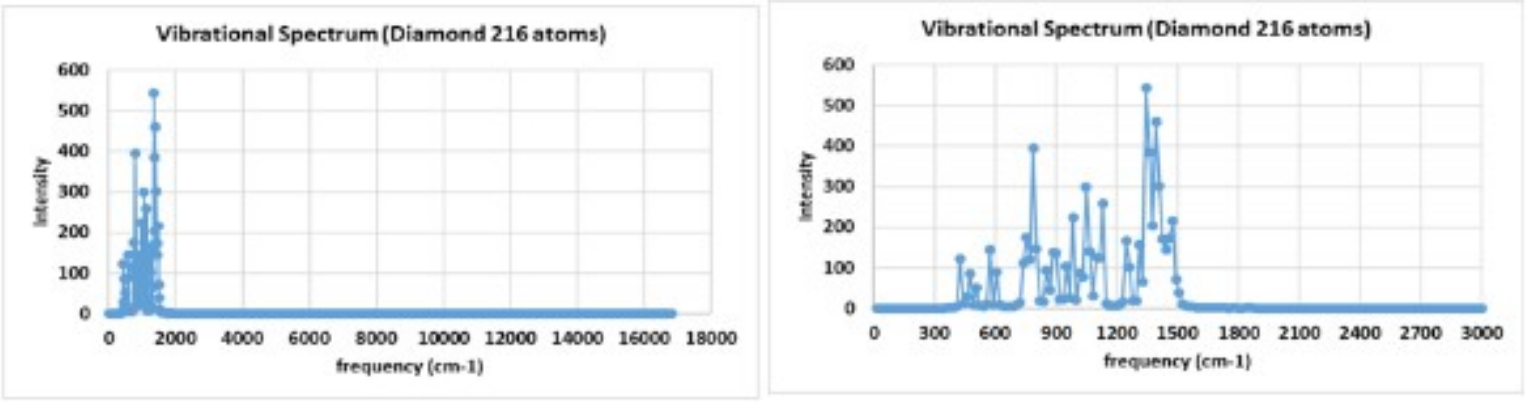

Figure 3.9.6: Vibrational spectrum of Diamond

NVT 10K simulation: T = 10.248795K

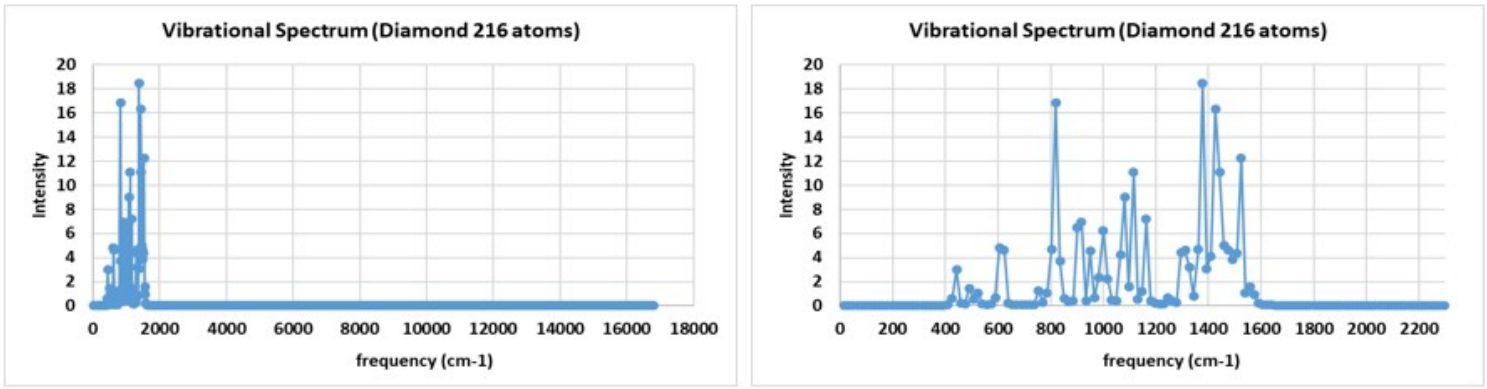

Figure 3.9.7: Vibrational spectrum of Diamond

According to [29], graphene has a vibrational mode at 1580cm^{-1} and diamond at 1332cm^{-1}. From Figure 3.9.4 and 3.9.5, we have peaks at 1671,6 and 1688,0cm^{-1} respectively. For the diamond structure of 216 atoms we see from Figure 3.9.6 and 3.9.7 peaks at 1475,0 and 1524,2cm^{-1}. In both structures, there is an overestimation of the potential. All the extra peaks correspond to other vibrational frequencies due to the various motions in the structure, which we will not study further.

Zigzag Graphene Nanoribbon (GNR): NVT simulation: T = 304.7113K

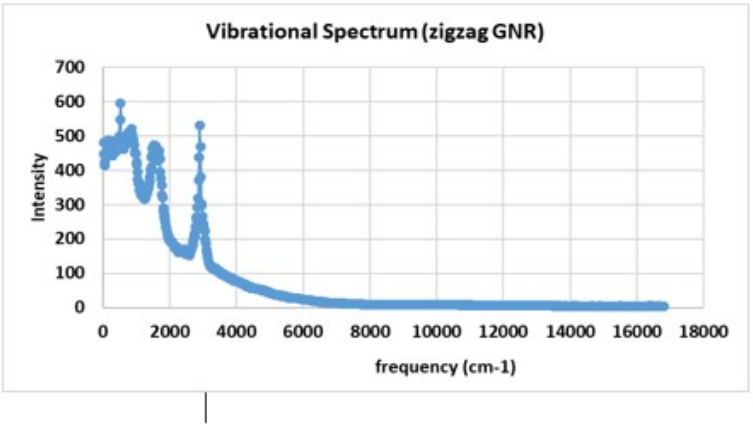

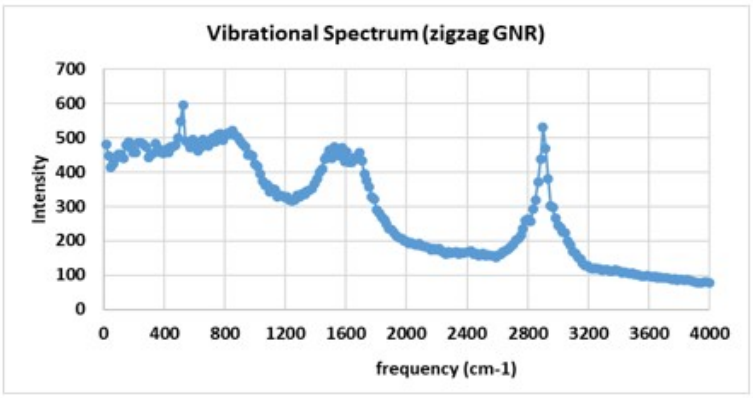

Figure 3.9.8: Vibrational spectrum of zigzag Graphene Nanoribbon

According to Figure 8 from [28], there are three regions of the experimental vibrational frequencies in zigzag graphene nanoribbons: (a) 600–1000 cm^{-1}. (b) 1000–1800 cm^{-1} and (c) 2950–3150cm^{-1}. More specifically there are peaks at 728, 742, 885, 957, 1147, 1317, 1448, 1531, 1621 and 3052cm^{-1}. In our case of zigzag GNR (width 10), in the graph of Figure 3.9.8 we note peaks at 524,4 cm^{-1}, between 1458,6 and 1704,4 cm^{-1}, and at 2900,8 cm^{-1}.

Localized excitations

First we changed the position of one specific hydrogen for 0,01Å by hand in each minimized structure and did a NVE simulation. Then we stored the velocities (vx, vy, vz) of each atom and for each component we did FFT. We keep N=2048 points.

- **Methane (CH_4)**

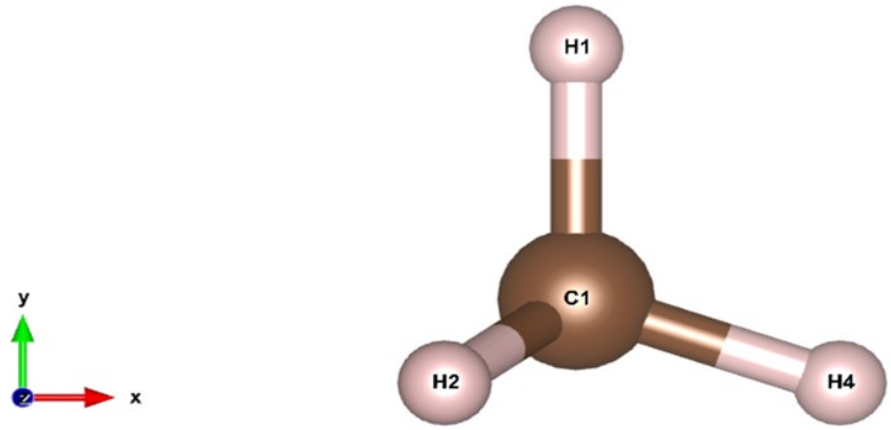

We displace Hydrogen 1 (H_1 – atom2) for 0,01Å in the y-axis. Below we can see the vibrational spectrum for Methane.

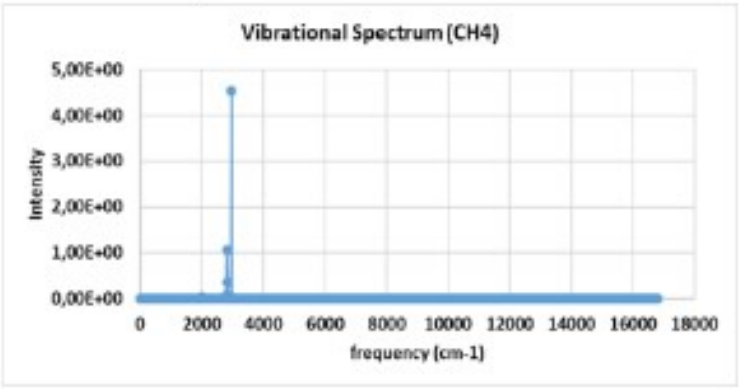

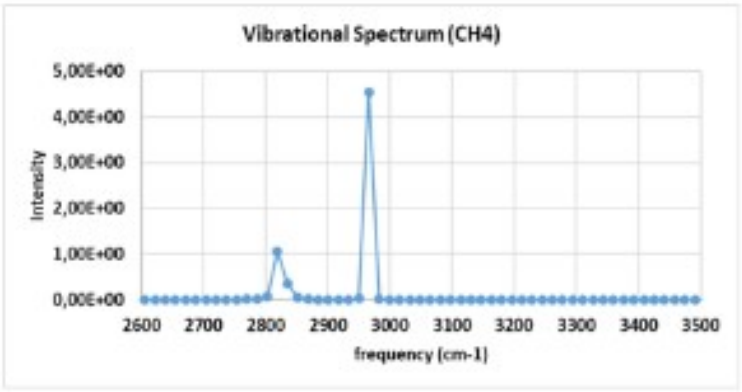

Figure 3.9.9: Vibrational spectrum of methane molecule

The first peak at 2818,86cm^{-1} corresponds to the antisymmetric stretch and the larger one, 2966,36cm^{-1}, to the symmetric stretch

Peak	Frequency (Hz)	Frequency (cm^{-1})
1	8,39844*10^{13}	2818,86
2	8,83789*10^{13}	2966,36

- **Benzene (C_6H_6)**

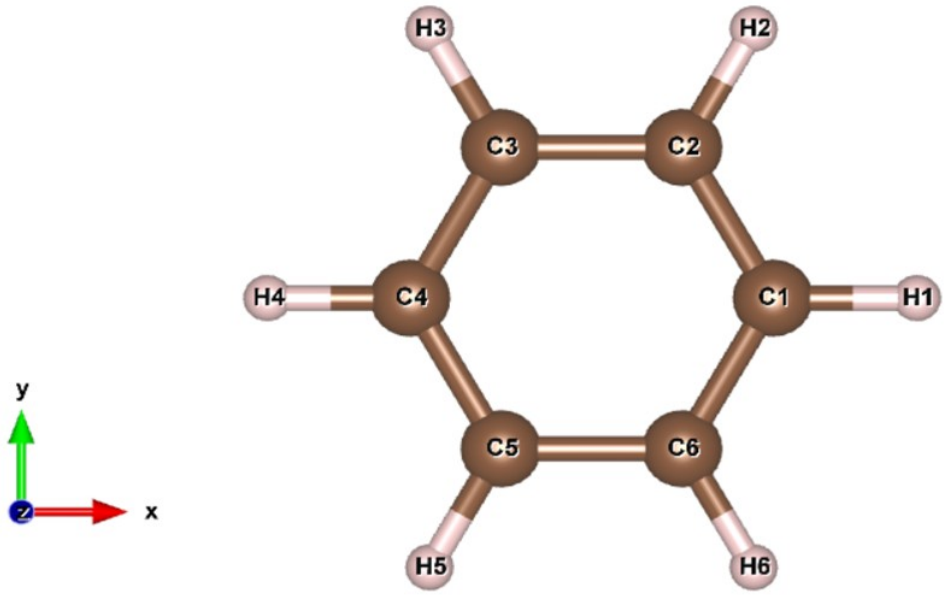

We displace Hydrogen 1 (H_1 – atom7) for 0,01Å in the x-axis.

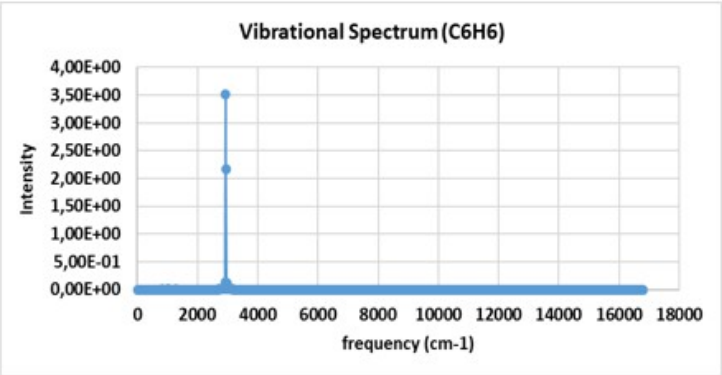

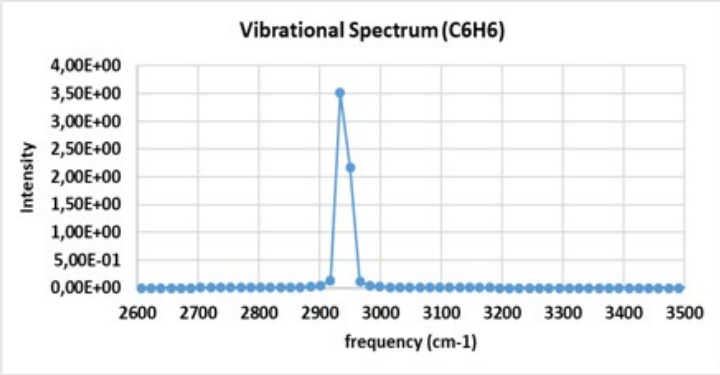

Figure 3.9.10: Vibrational spectrum of benzene molecule

Peak	Frequency (Hz)	Frequency (cm^{-1})
1	$8{,}74023*10^{13}$	2933,58
2	$8{,}78906*10^{13}$	2949,97

- **$C_{22}H_{24}$**

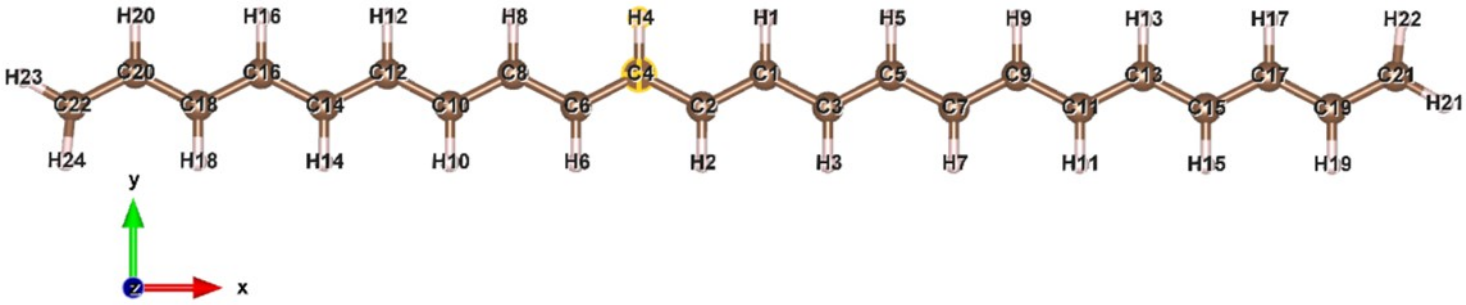

We displace Hydrogen 4 (H_4 – atom26) for 0,01Å in the y-axis. Below we can see the vibrational spectrum for $C_{22}H_{24}$.

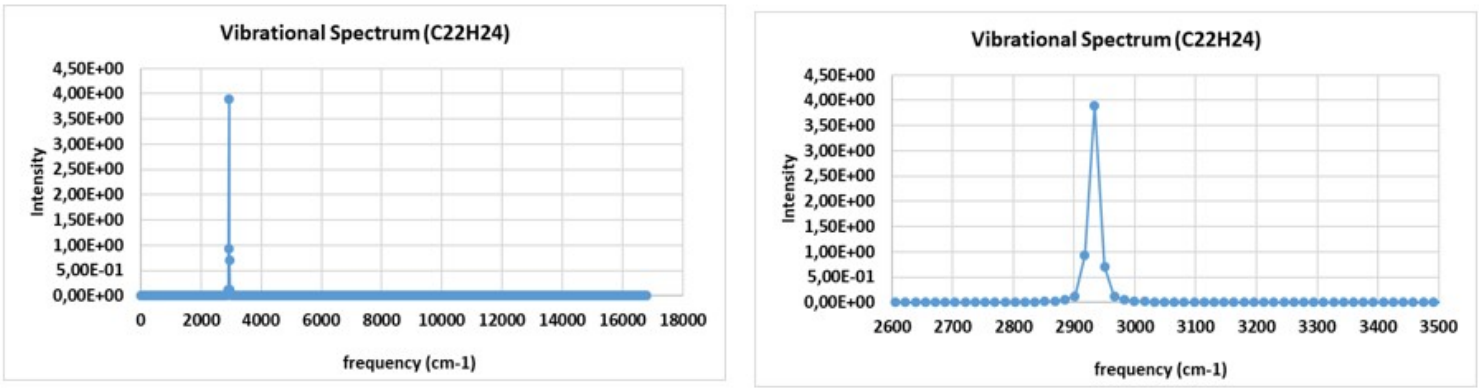

Figure 3.9.11: Vibrational spectrum of C22H24

Peak	Frequency (Hz)	Frequency (cm^{-1})
1	$8{,}74023*10^{13}$	2933,58

- **Zigzag Graphene Nanoribbon (width10)**

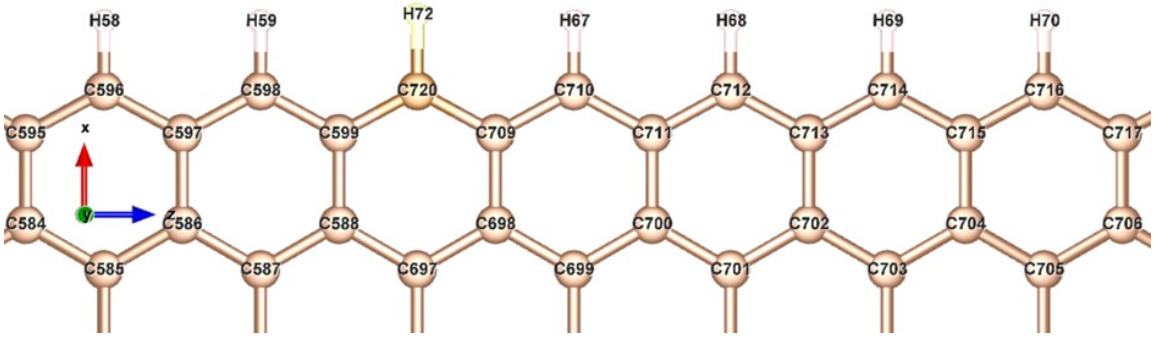

We displace Hydrogen 72 (H_{72} – atom792) for 0,01Å in the x-axis. Below we can see the vibrational spectrum of zigzag GNR (width 10).

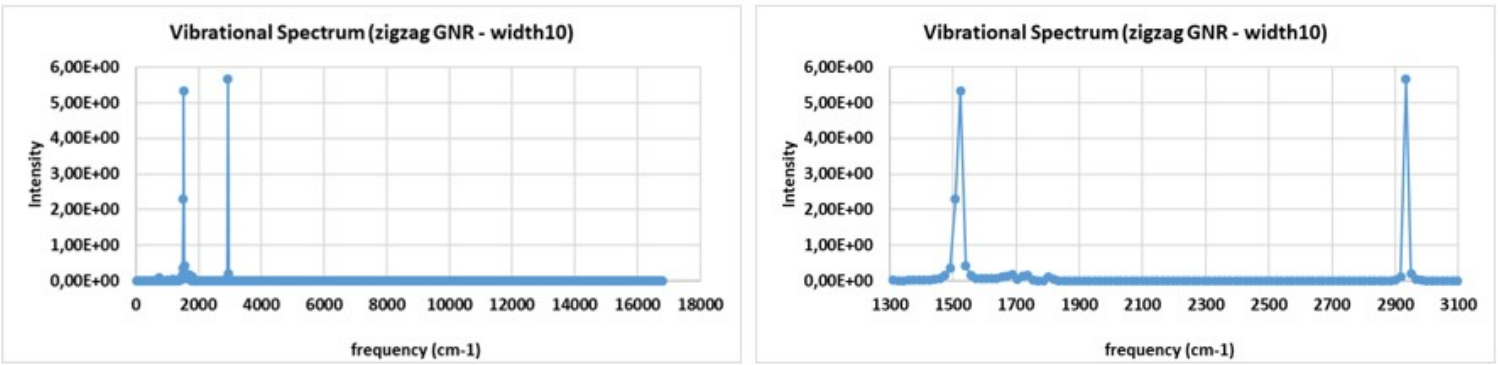

Figure 3.9.12: Vibrational Spectrum of zigzag GNR

The first peak at 1524,15cm^{-1} corresponds to the antisymmetric stretch and the larger one, 2933,58cm^{-1}, to the symmetric stretch.

Localized vibrational modes

- ## Methane

Displacement of atom 2 (H_1) in Methane for 0,1Å - Δx vs Time graph

First we move hydrogen H_1 by Δx=0,1Å up and do NVE simulation. After 10ps we see in the graph below the displacement along the y-axis as a function of time for hydrogen 1 and 2.

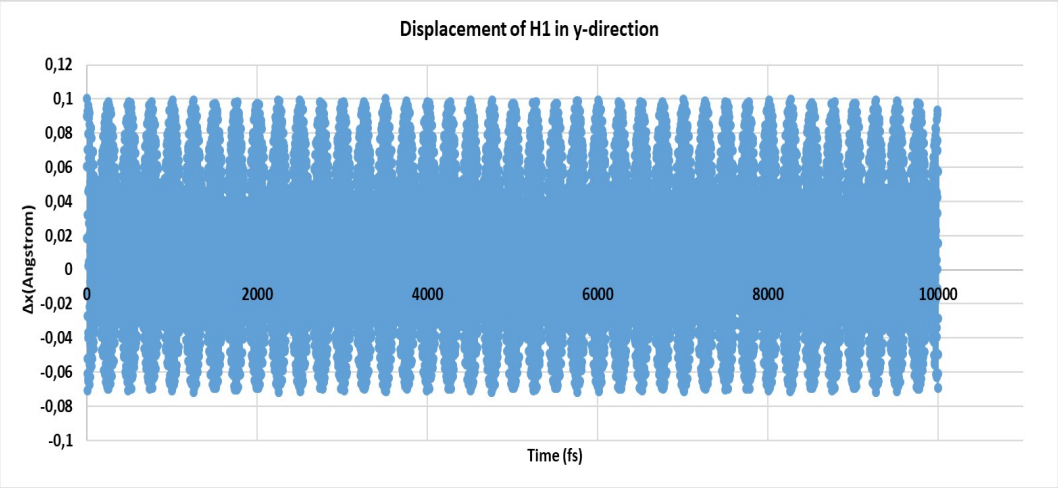

Figure 3.9.13: Displacement of atom H1 in the y-direction from the equilibrium position when H1 is initially displaced by Δx=0.1 Å vs. time

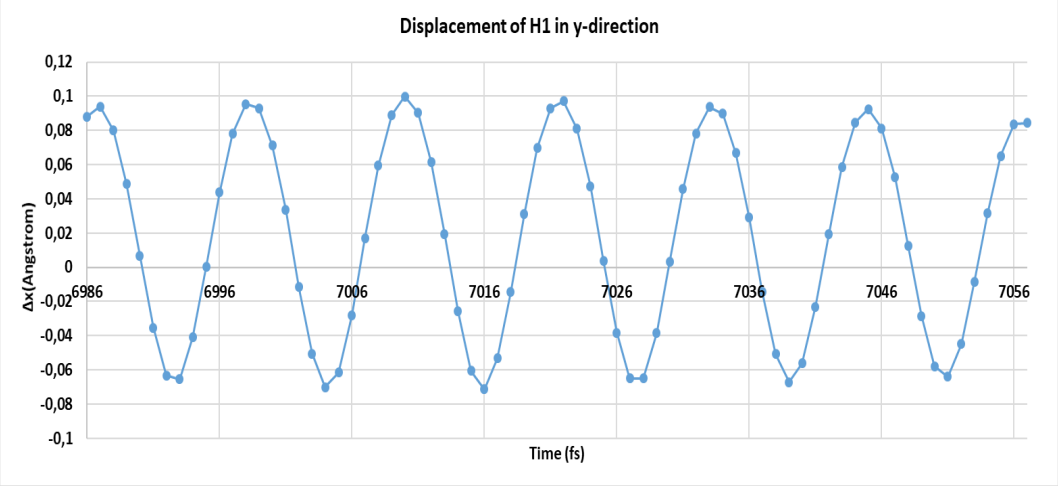

Figure 3.9.14: Displacement of atom H1 in the y-direction from the equilibrium position when H1 is initially displaced by Δx=0.1 Å vs. time for a short time interval (from 6,986ps to 7,057ps).

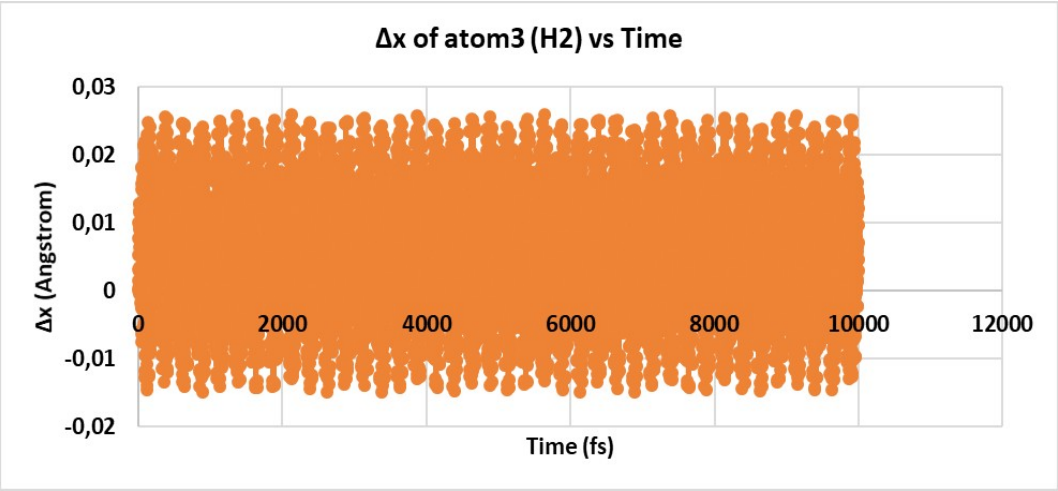

Figure 3.9.15: Displacement of atom H2 in the y-direction from the equilibrium position when atom H1 is initially displaced by Δx=0.1 Å vs. time

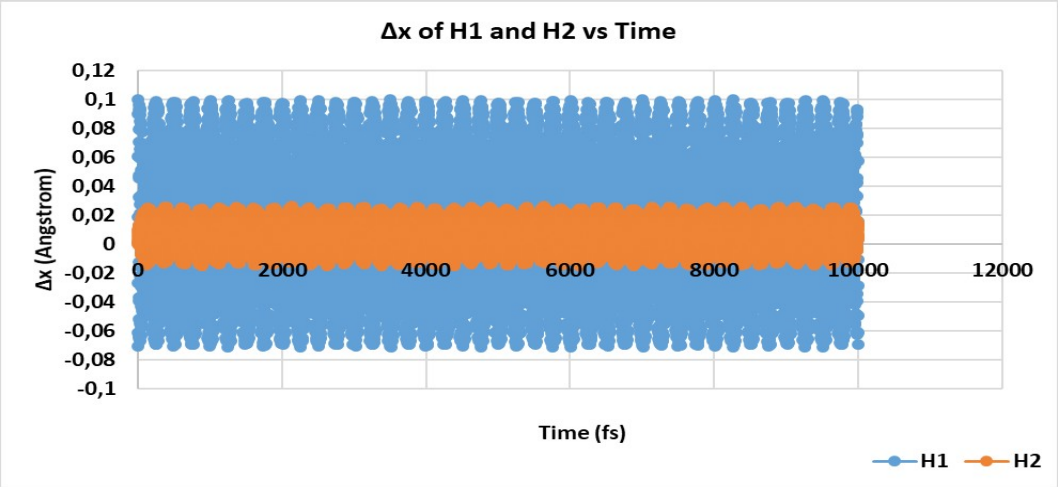

Figure 3.9.16: Displacements of the H-atoms in the y-direction from the equilibrium position when atom 1 is initially displaced by Δx=0.1 Å vs. time

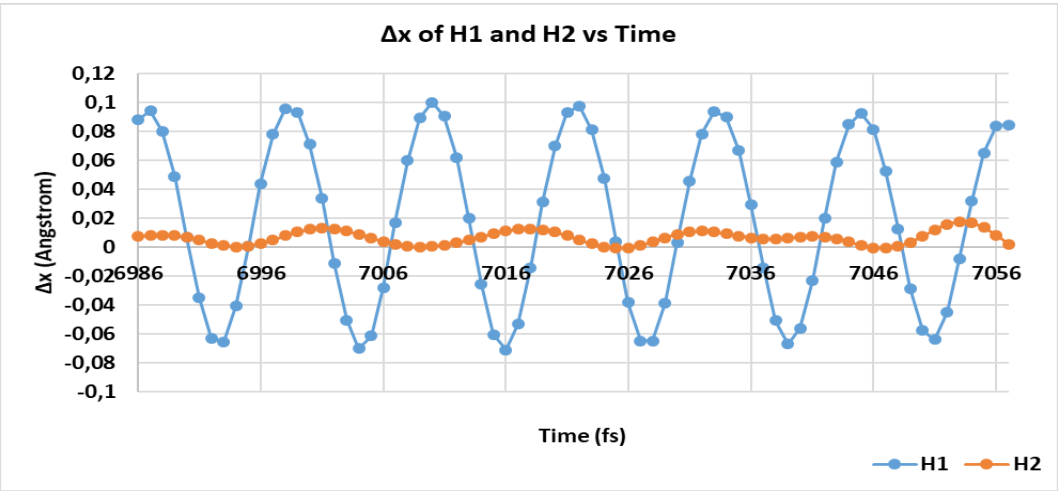

Figure 3.9.17: Displacements of the H-atoms in the y-direction from the equilibrium position when atom 1 is initially displaced by Δx=0.1 Å vs. time for a short time interval (from 6,986ps to 7,057ps).

From Figure 3.9.17 we calculate first the period (T=12fs) and then the frequency at 2797,01cm^{-1}. In the section before we calculated the frequency by changing the position for Δx=0,01Å and had two peaks, one at 2818,86cm^{-1} and the other at 2966,36cm^{-1}. The difference between the results is maybe based on the Δx factor. In the next structure we will displace the hydrogen for 0,1Å and for 0,01Å for better comparisons.

- **Benzene**

Displacement of atom 2 (H_1) in Benzene for 0,1Å - Δx vs Time graph

First we move hydrogen H_1 by Δx = 0,1Å to the right and do NVE simulation. After 10ps we see in the graph below the displacement along the x-axis as a function of time for hydrogen 1 and 3.

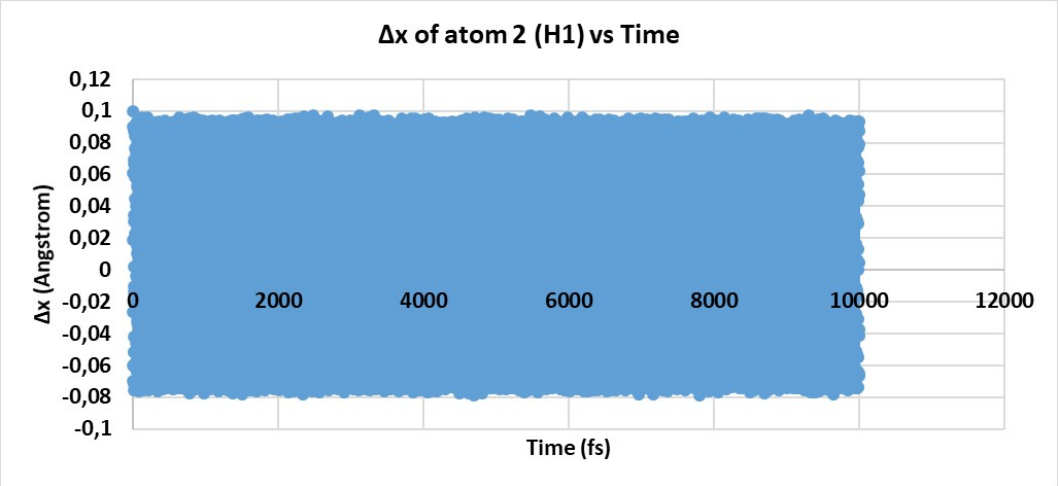

Figure 3.9.18: Displacement of atom H1 in the x-direction from the equilibrium position when H1 is initially displaced by Δx=0.1 Å vs. time

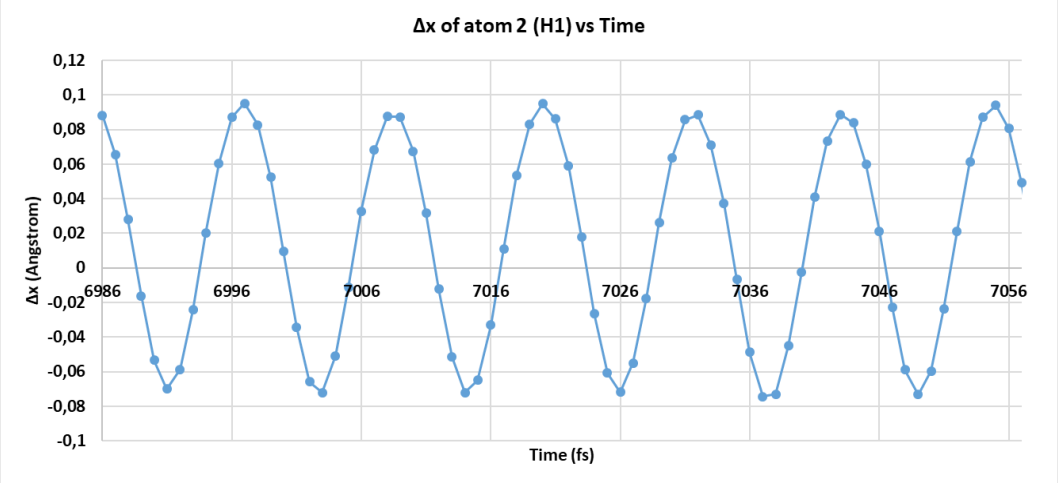

Figure 3.9.19: Displacement of atom H1 in the x-direction from the equilibrium position when H1 is initially displaced by Δx=0.1 Å vs. time for a short time interval (from 6,986ps to 7,057ps).

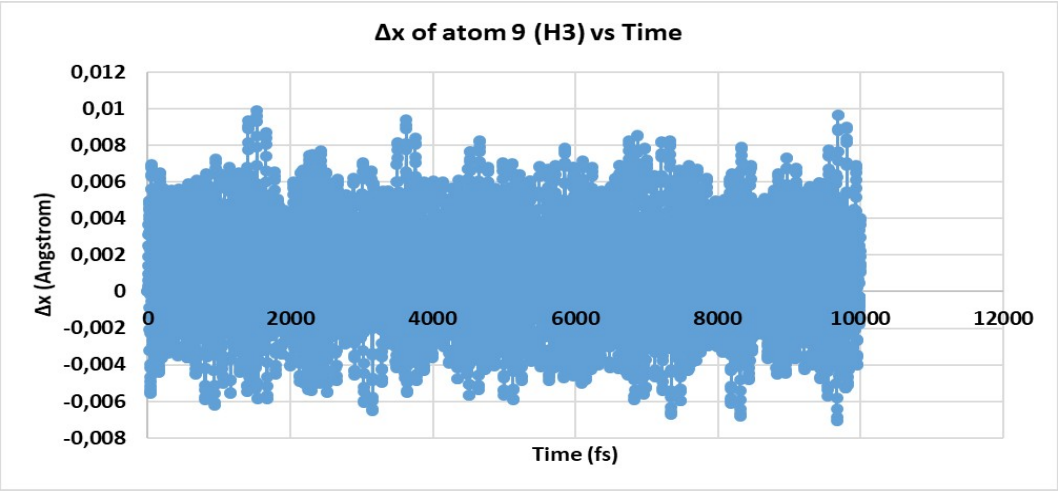

Figure 3.9.20: Displacement of atom H3 in the x-direction from the equilibrium position when H1 is initially displaced by Δx=0.1 Å vs. time

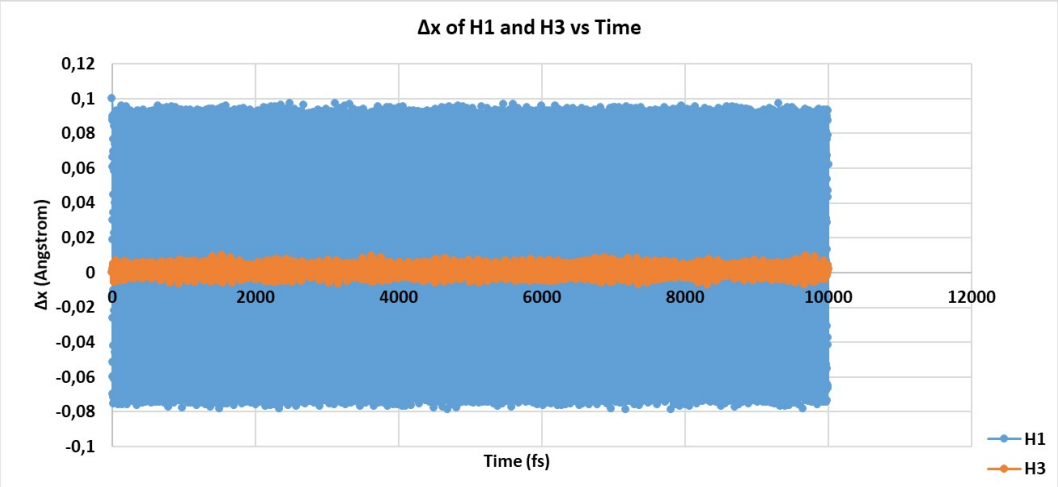

Figure 3.9.21: Displacements of the H-atoms in the x-direction from the equilibrium position when H1 is initially displaced by Δx=0.1 Å vs. time

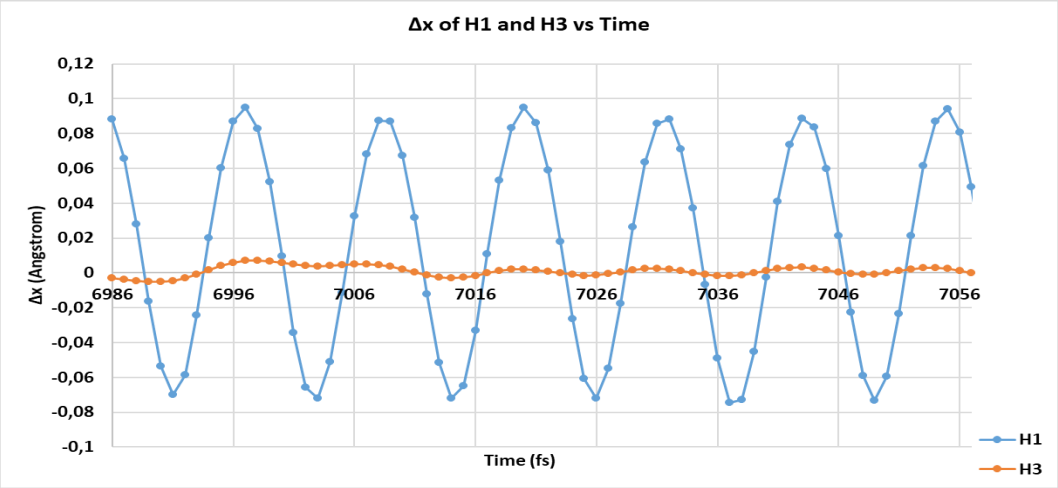

Figure 3.9.22: Displacements of the H-atoms in the x-direction from the equilibrium position when atom 1 is initially displaced by Δx=0.1 Å vs. time for a short time interval (from 6,986ps to 7,057ps).

From Figure 3.9.22 the frequency is calculated 2797,01 cm^{-1}.

Displacement of atom 2 (H_1) in Benzene for 0,01Å - Δx vs Time graph

First we move hydrogen H_1 by Δx = 0,01Å to the right and do NVE simulation. After 10ps we see in the graph below the displacement along the x-axis as a function of time for hydrogen 1 and 3.

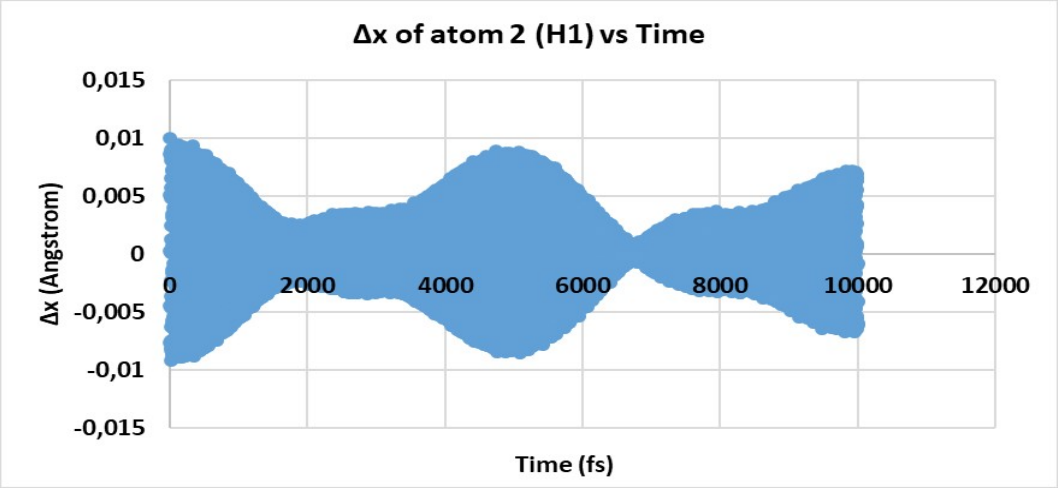

Figure 3.9.23: Displacement of atom H1 in the x-direction from the equilibrium position when H1 is initially displaced by Δx=0.01 Å vs. time

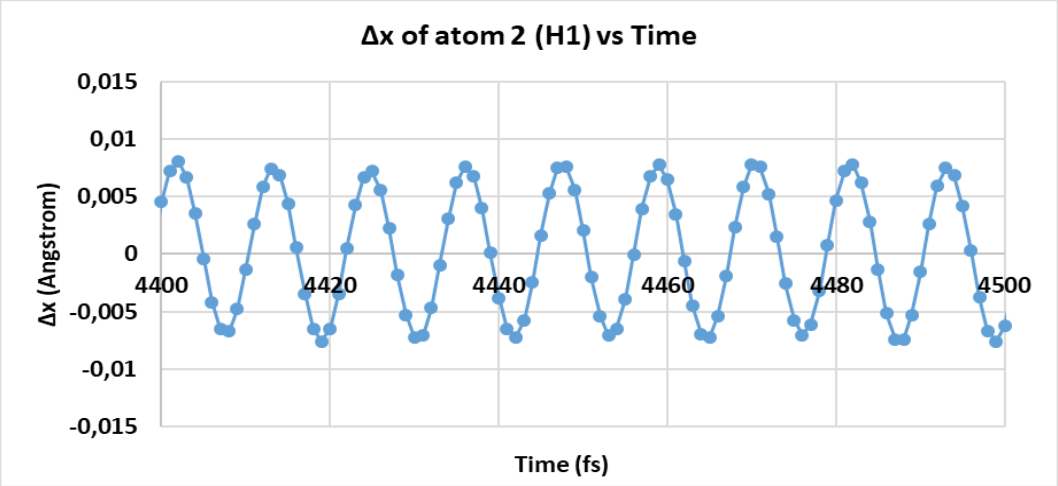

Figure 3.9.24: Displacement of atom H1 in the x-direction from the equilibrium position when H1 is initially displaced by Δx=0.01 Å vs. time for a short time interval (from 4,400ps to 4,500ps).

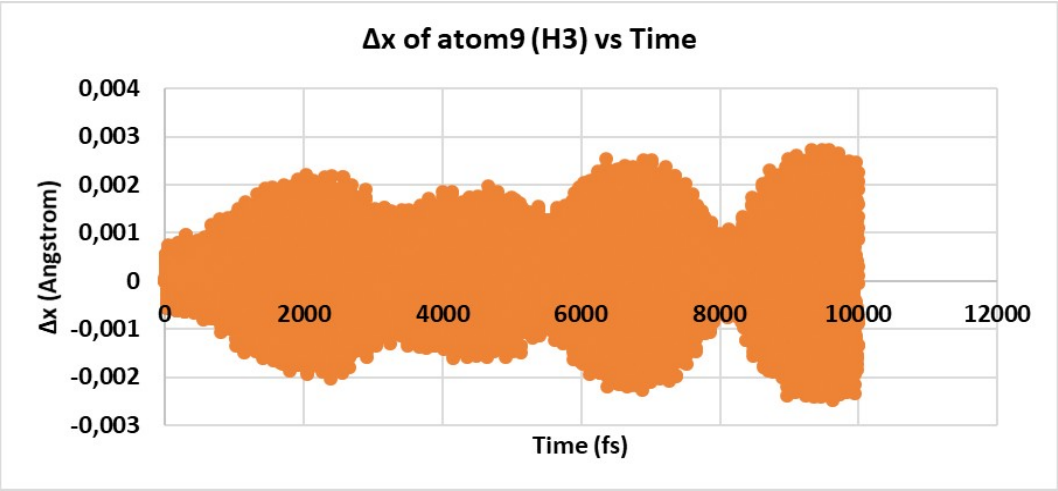

Figure 3.9.25: Displacement of atom H3 in the x-direction from the equilibrium position when H1 is initially displaced by Δx=0.01 Å vs. time

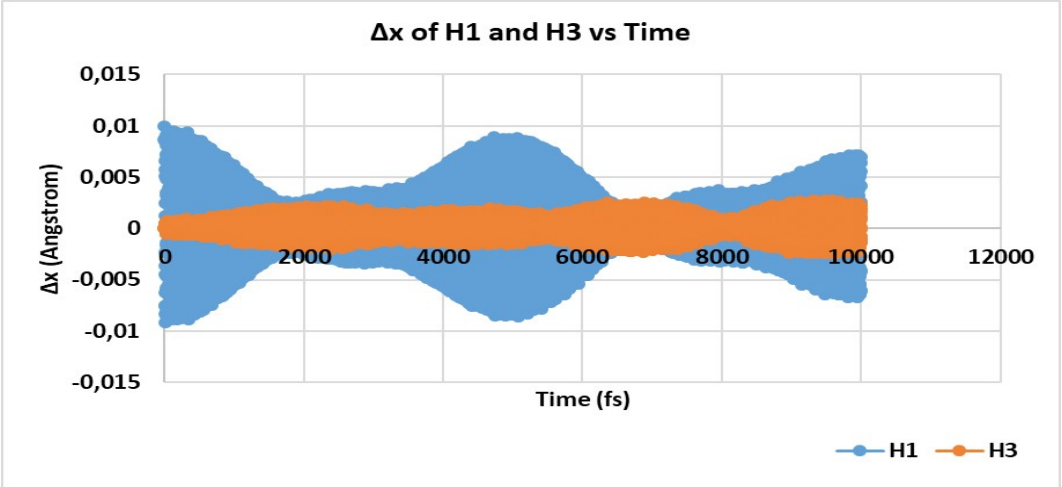

Figure 3.9.26: Displacements of the H-atoms in the x-direction from the equilibrium position when H1 is initially displaced by Δx=0.01 Å vs. time

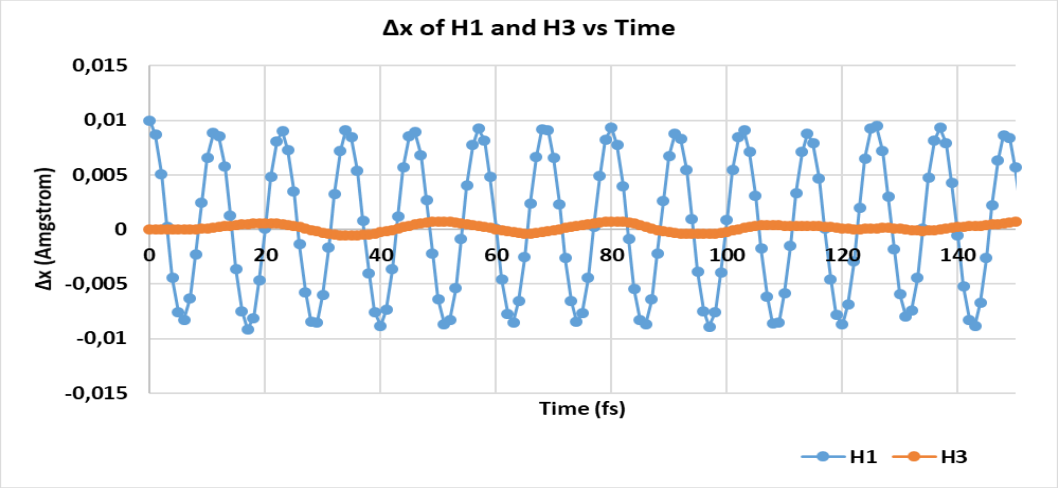

Figure 3.9.27: Displacements of the H-atoms in the x-direction from the equilibrium position when atom 1 is initially displaced by Δx=0.01 Å vs. time for a short time interval (from 0,000ps to 0,150ps).

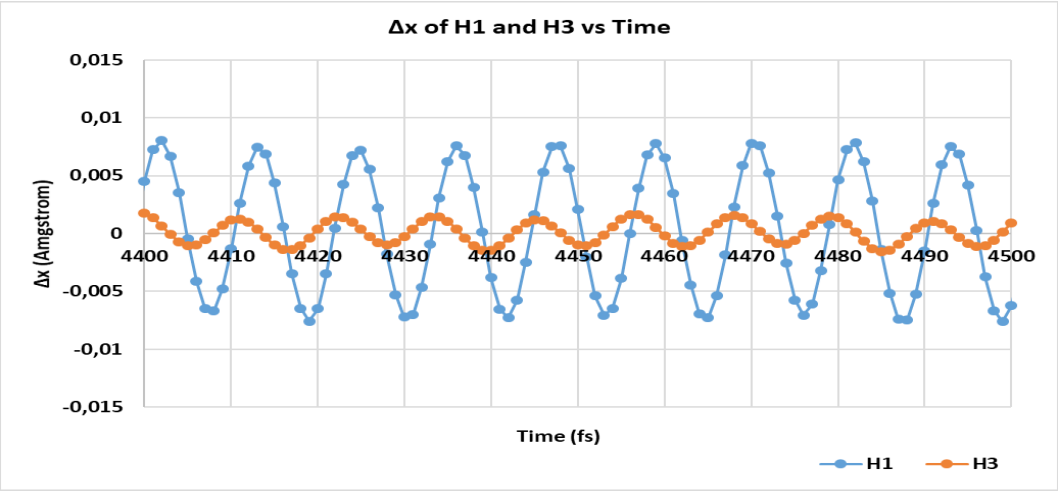

Figure 3.9.28: Displacements of the H-atoms in the x-direction from the equilibrium position when atom 1 is initially displaced by Δx=0.01 Å vs. time for a short time interval (from 4,400ps to 4,500ps).

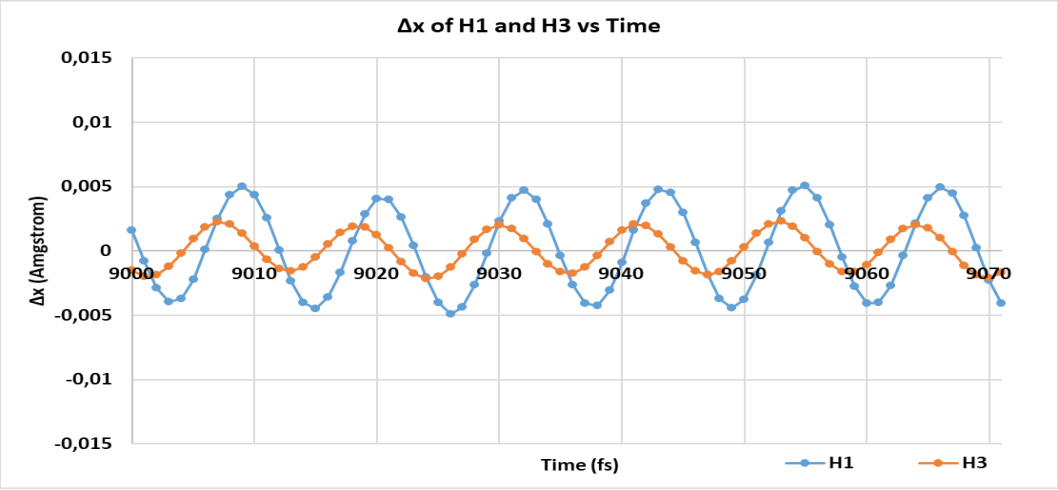

Figure 3.9.29: Displacements of the H-atoms in the x-direction from the equilibrium position when atom 1 is initially displaced by Δx=0.01 Å vs. time for a short time interval (from 9,000ps to 9,071ps).

We know that: $f=\frac{1}{T}\ (1)$ and from the diagram in Figure 3.9.29 we calculate the period: $T=9026\,fs-9015\,fs=11\,fs=11\times10^{-15}\,sec$

Therefore, from relation (1) it follows that:

$$f=\frac{1}{11\times10^{-15}\,sec}=0{,}0909090909\times10^{15}\,Hz$$

And we convert frequency from Hz to cm^{-1}:

$$f=0{,}0909090909\times10^{15}\times3{,}35641\times10^{-11}\simeq3051{,}28\ \ cm^{-1}\ (2)$$

For benzene, four different ways were used to calculate vibrational frequencies. First we used Fast Fourier Transform (FFT) and molecular dynamics (MD) at 300K where the atoms acquired random velocities and positions. In the second case we manually moved a specific hydrogen by Δx=0,01Å and obtained the frequency spectrum from FFT. In the first method we calculate a frequency of 2917,17cm^{-1} and in the second one 2933,58 cm^{-1}. So there is a percentage difference of 0.6%. Then we moved the hydrogen again by hand by Δx=0,1Å and Δx=0,01Å and from the displacement-time diagram we calculated first the period and then the frequency. In both of the latter cases we do not observe satisfying results, as one value (2797,01cm^{-1}) is lower than the experimental values (2800–3200 cm^{-1}), while the other is higher (3051,28cm^{-1})compared to the previous values we calculated.

- **C22H24**

Displacement of atom 26 (H_4) in C22H24 for 0,1Å - Δx vs Time graph

First we move hydrogen H_4 by Δx = 0,1Å up and do NVE simulation. After 10ps we see in the graph below the displacement along the y-axis as a function of time for hydrogen 4 and 18.

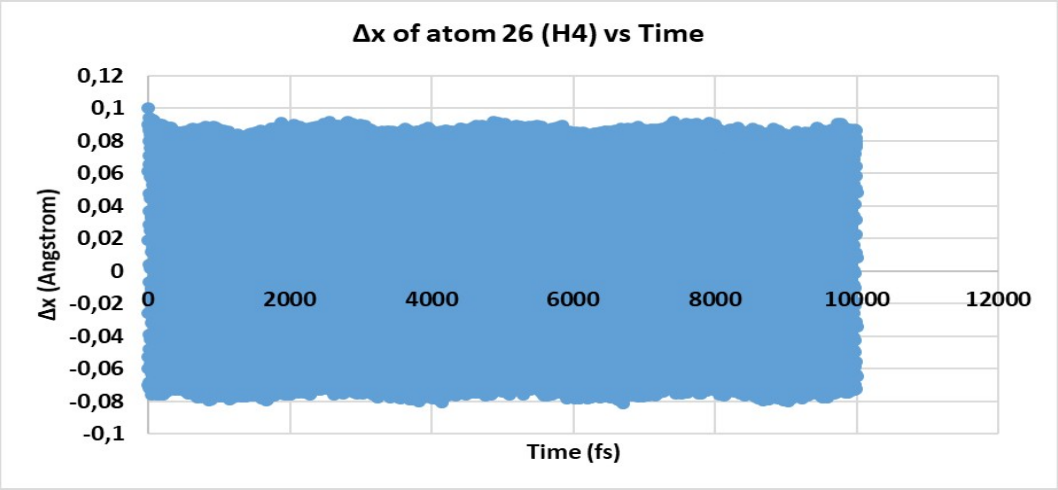

Figure 3.9.30: Displacement of atom H4 in the y-direction from the equilibrium position when H4 is initially displaced by Δx=0.1 Å vs. time

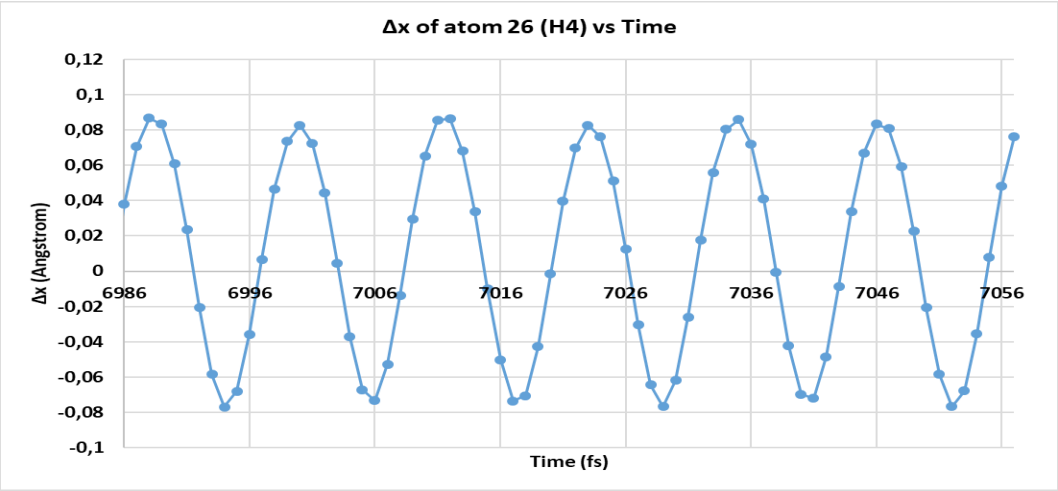

Figure 3.9.31: Displacement of atom H4 in the y-direction from the equilibrium position when H4 is initially displaced by Δx=0.1 Å vs. time for a short time interval (from 6,986ps to 7,057ps).

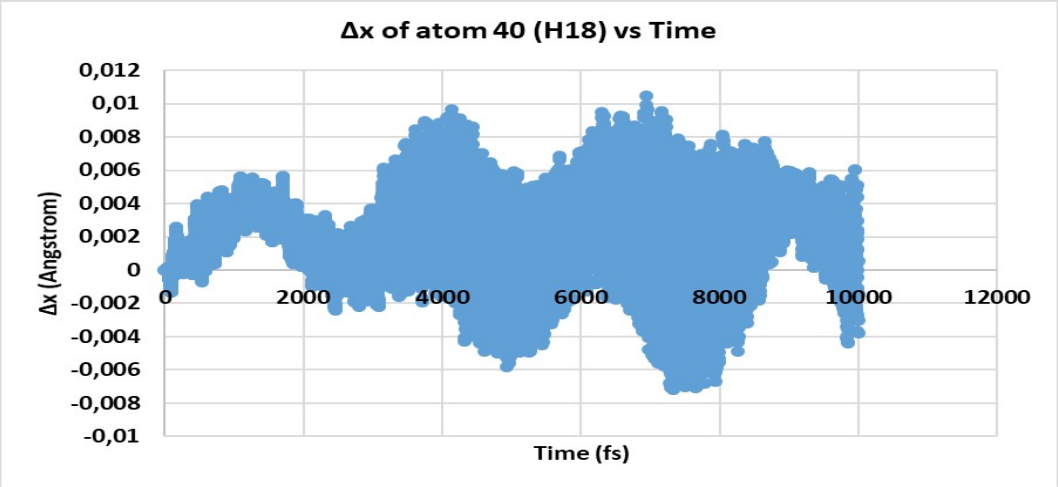

Figure 3.9.32: Displacements of atom H18 in the y-direction from the equilibrium position when atom 4 is initially displaced by Δx=0.1 Å vs. time

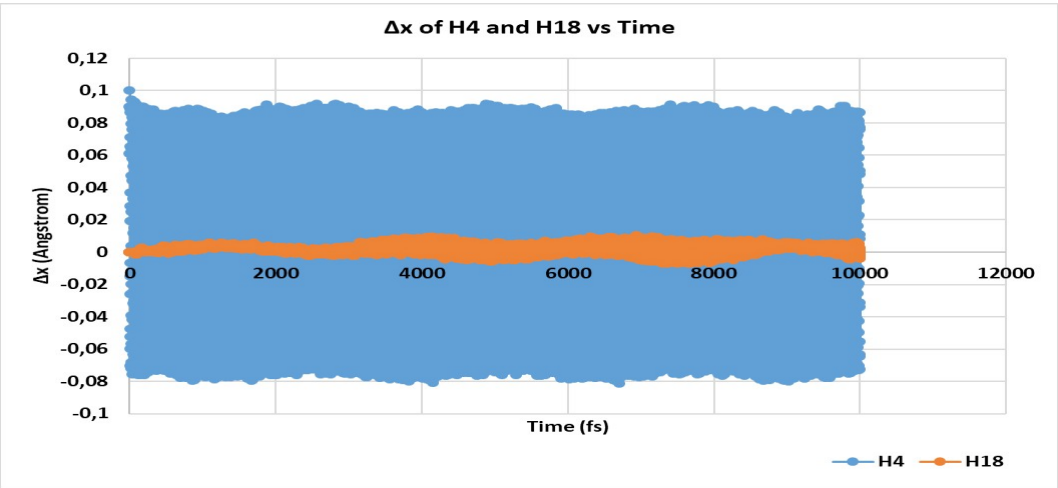

Figure 3.9.33: Displacements of the H-atoms in the y-direction from the equilibrium position when H4 is initially displaced by Δx=0.1 Å vs. time

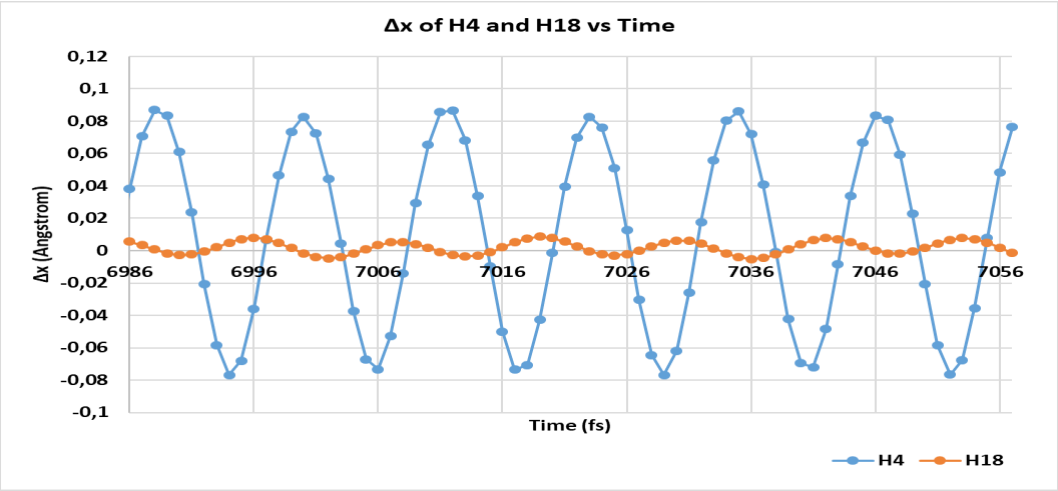

Figure 3.9.34: Displacements of the H-atoms in the y-direction from the equilibrium position when atom 4 is initially displaced by Δx=0.1 Å vs. time for a short time interval (from 6,986ps to 7,057ps).

- **Zigzag Graphene Nanoribbon (width 10)**

Displacement of atom 792 (H_{72}) in zigzag Graphene Nanoribbon (width 10) for 0,1Å - Δx vs Time graph

First we move hydrogen H_{72} by Δx = 0,1Å in the x-axis and do NVE simulation. After 10ps we see in the graph below the displacement along the x-axis as a function of time for hydrogen 72 and 40.

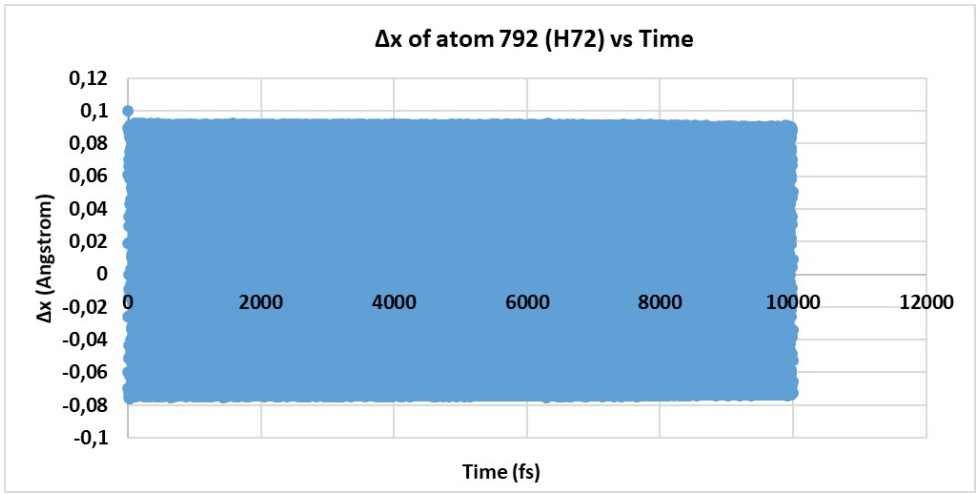

Figure 3.9.35: Displacement of atom H72 in the x-direction from the equilibrium position when H72 is initially displaced by Δx=0.1 Å vs. time

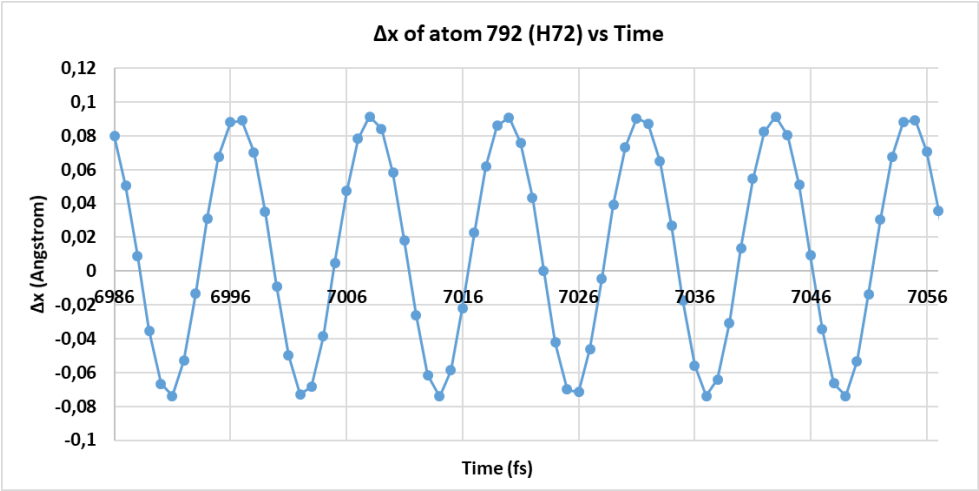

Figure 3.9.36: Displacement of atom H72 in the y-direction from the equilibrium position when H72 is initially displaced by Δx=0.1 Å vs. time for a short time interval (from 6,986ps to 7,057ps).

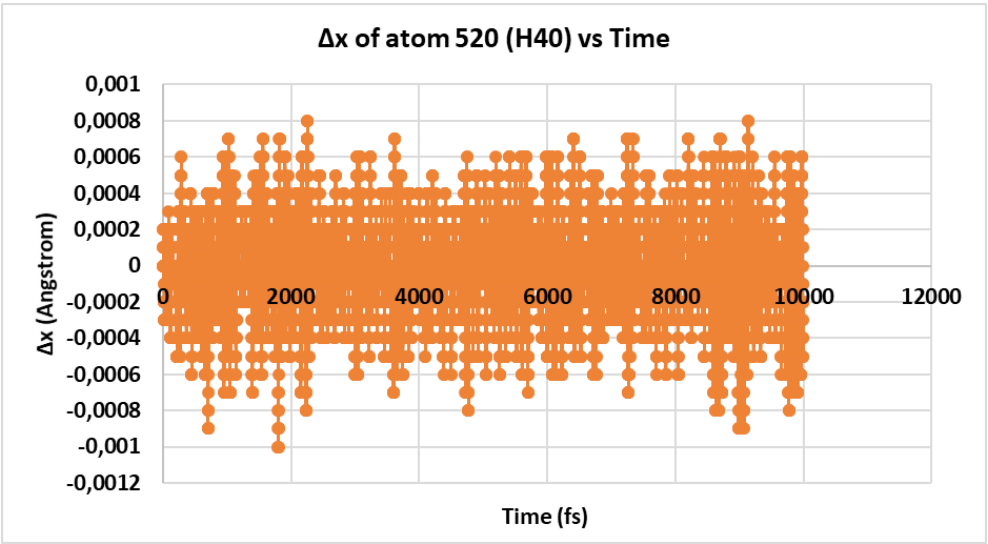

Figure 3.9.37: Displacements of atom H40 in the x-direction from the equilibrium position when atom72 is initially displaced by Δx=0.1 Å vs. time

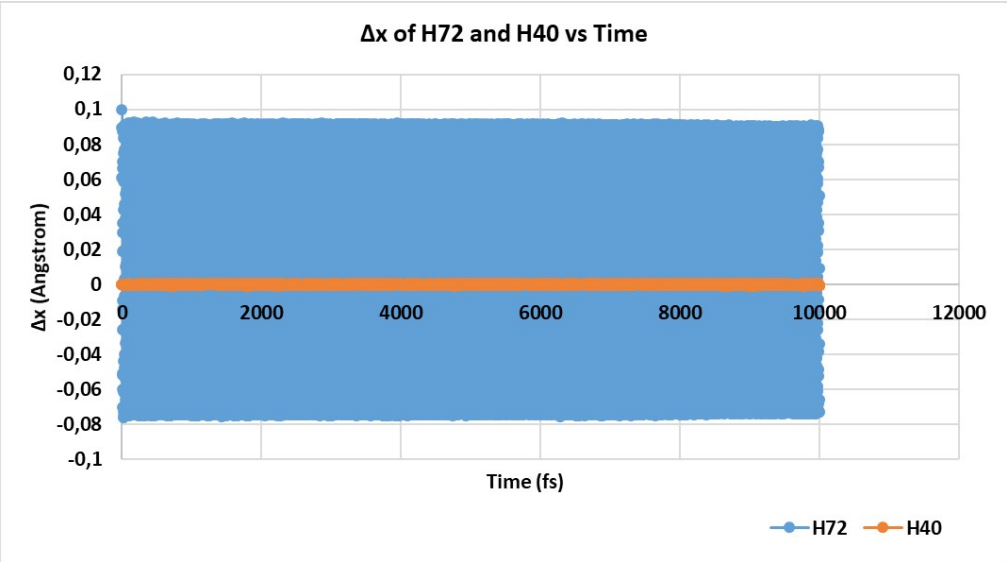

Figure 3.9.38: Displacements of the H-atoms in the x-direction from the equilibrium position when H72 is initially displaced by Δx=0.1 Å vs. time

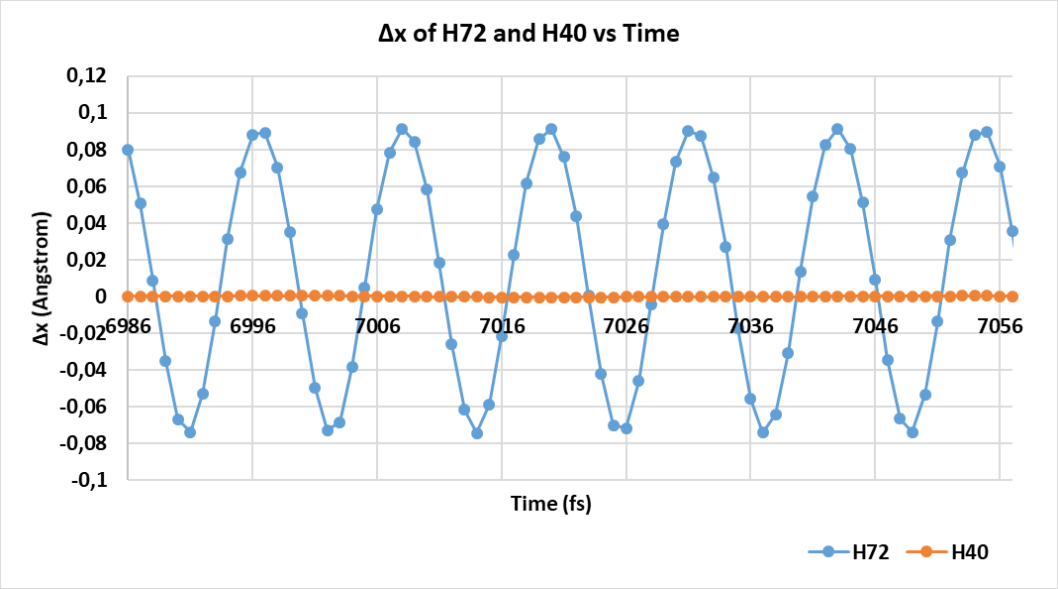

Figure 3.9.39: Displacements of the H-atoms in the y-direction from the equilibrium position when atom 72 is initially displaced by Δx=0.1 Å vs. time for a short time interval (from 6,986ps to 7,057ps).

In Figure 3.9.28 and 3.9.39 of zigzag GNR, the Δx of H_{40} appears to be almost zero. This means that the oscillation does not spread in the structure.

Chapter 4: Conclusions

Conclusions

Ab initio and classical molecular dynamics simulations, on materials that are composed of carbon and hydrogen, are performed to characterize lattice constants, bond lengths and other basic properties. An additional goal was to get and understand the vibrational spectra of these structures. The main conclusions from this work are as follow. After creating the diamond and graphene structures, we started our calculations using DFT, the classical empirical Brenner and Tersoff potentials and lastly the cg algorithm of LAMMPS together with the RDF function to see if there are differences in the calculation of the lattice constant. As the results demonstrated, we noticed that for diamond the lattice constants calculated by the classical dynamics and the cg algorithm (RDF) were closer to the experimental value (3.57Å) while in the graphene structure there is a major disagreement with the Tersoff potential. All subsequent simulations were performed by applying the Brenner Potential. Afterwards, the additional oscillation of the atoms with increasing temperature from 10 to 300 Kelvin was observed with RDF. We continued our study focusing on the bonds and angles in methane, benzene molecules and the hydrocarbon chains. The experimental and theoretical results are in agreement, but we noticed something unusual in the chain $C_{22}H_{24}$. The double and single carbon-carbon bond had the same length, which we did not expect, since the double bond at the right edge of $C_{22}H_{44}$ remained unchanged. We wanted to further investigate this and applied the RDF function to zigzag and armchair graphene nanoribbons for width 4,6,10 and 20 in each case. We detect in the case of the armchair GNR a slight difference in the values, but the constant remains the same for each width in the zigzag GNR structure. When we studied the bonds in a more detailed way, we realized that the bonds in the outer carbons are shorter. In the Armchair GNR we have values of 1.38Å and 1.40Å, while in the Zigzag GNR 1.40Å. In both cases all other C-C bonds are 1.42Å, as the experimental value. The latter calculations are based on the vibrational spectra and localized excitations of all structures. We noted that the Brenner Potential is also reliable for most vibrational spectra, in overall qualitative agreement with experiment, but underestimates C-H stretch and overestimates C-C vibration frequencies. Except for normal modes obtained after thermalization, we examined how initially localized C-H vibration evolves with time. Regarding to the localized vibrational modes, when we excited H_1 with a large initial amplitude of 0,1Å for methane, benzene, $C_{22}H_{24}$ and zigzag GNR structures, we observed the non-linear effect. This indicates that the vibration remains localized on the C-H_1 bond, as shown in Figures 3.9.17 - 3.9.22 - 3.9.34 and 3.9.39 for each structure respectively. In Figure 3.9.26 of benzene molecule, we excited hydrogen H_1 with a small initial amplitude of 0,01Å and after about 2ps hydrogen H_3 vibrates with an amplitude of the same order of magnitude, which means that energy spreads to other C-H bonds as expected. Figure 3.9.27 is misleading as vibration is localized at C-H_1, because it is for short initial time interval, but it spreads as time goes by.

5.Bibliography

[1] Wikipedia: Graphene

[2] Bergmann and Machado, 2015

Nanotechnology: Future of Environmental Air Pollution Control

Elham F. Mohamed (Corresponding author) - Air Pollution Department, Division of Environment

[3]https://bio.libretexts.org/Bookshelves/Introductory_and_General_Biology/Book%3A_General_Biology_(Boundless)/02%3A_The_Chemical_Foundation_of_Life/2.19%3A__Carbon_-_Hydrocarbons

[4]Wikipedia: Diamond

[5]Wikipedia: Radial distribution function

[6]Wikipedia: Bond order potential

[7] https://nanohub.org/resources/1167/download/2006.03.29-hsu-v03.pdf

[8] Encyclopedia of Condensed Matter Physics 2005, Pages 395-402

Density-Functional Theory S.Kurth M.A.L. Marques E.K.U. Gross

[9] Brenner, D.W.; 'Empirical potential for hydrocarbons for use in simulating the chemical vapor deposition of diamond films', Physical - Review B, vol. 42, no. 15, pp. 9458-9471, July 1990

[10] Wikipedia: Molecular dynamics

[11] LAMMPS Documentation (3 Aug 2022 version)

[12] The atomic simulation environment—a Python library for working with atoms - Ask Hjorth Larsen1,2, Jens Jørgen Mortensen3, Jakob Blomqvist4, Ivano E Castelli5, Rune Christensen6, Marcin Dułak3, Jesper Friis7, Michael N Groves8, Bjørk Hammer8, Cory Hargus

[13] Near infrared spectroscopy as a diagnostic tool in surveillance of arboviral vector control, predicting Wolbachia infection in post-mortem Aedes aegypti. By: Mathijs Mutsaers

[14]Wikipedia: Molecular vibration

[15] NUMERICAL RECIPES IN FORTRAN 77: THE ART OF SCIENTIFIC COMPUTING (ISBN 0-521-43064-X) Second Edition

[16] Liangzhen Zheng, Yuguang Mu, in Encyclopedia of Bioinformatics and Computational Biology, 2019

[17] Discrete breathers in realistic models: hydrocarbon structures: Author G.Kopidakis, S.Aubry

[18] Bottom-Up Synthesis and Electronic Structure of Graphene Nanoribbons on Surfaces

C. Bronner, in Encyclopedia of Interfacial Chemistry, 2018

[19] Polymers for Advanced Functional Materials

Y. Hernandez, K. Müllen, in Polymer Science: A Comprehensive Reference, 2012, 8.16.3 Graphene Nanoribbons

[20] LAMMPS - a flexible simulation tool for particle-based materials modeling at the atomic, meso, and continuum scales, A. P. Thompson, H. M. Aktulga, R. Berger, D. S. Bolintineanu, W. M. Brown, P. S. Crozier, P. J. in 't Veld, A. Kohlmeyer, S. G. Moore, T. D. Nguyen, R. Shan, M. J. Stevens, J. Tranchida, C. Trott, S. J. Plimpton, Comp Phys Comm, 271 (2022) 10817.

[21] Vibrational spectra of ammonia, benzene, and benzene adsorbed on Si (001) by first principles calculations with periodic boundary conditions - M. Preuss and F. Bechstedt - Institut für Festkörpertheorie und -optik, Friedrich-Schiller-Universität, 07743 Jena, Germany

[22] https://www.diamonds-only.gr/what-is-a-diamond/?lang=en

[23]https://chem.libretexts.org/Bookshelves/Organic_Chemistry/Supplemental_Modules_(Organic_Chemistry)/Fundamentals/Hybrid_Orbitals

[24] Wikipedia: Normal mode

[25] Wikipedia: Frequency domain

[26]https://www.physik.fuberlin.de/einrichtungen/ag/agreich/lehre/Archiv/ss2011/docs/GinaPeschel-Handout.pdf

[27] Evaluation and comparison of classical interatomic potentials through a user-friendly interactive web-interface - Kamal Choudhary, Faical Yannick P. Congo, Tao Liang, Chandler Becker, Richard G. Hennig & Francesca Tavazza

[28] Brominated positions on graphene nanoribbon analyzed by infrared spectroscopy-Yasuhiro Yamada, Shiori Masaki & Satoshi Sato - Journal of Materials Science volume 55, pages 10522–10542 (2020)

[29] Diamond-like amorphous carbon, J. Robertson - Engineering Department, Cambridge University, Cambridge CB2 1PZ, UK

[30] https://www.chem.purdue.edu/jmol/vibs/c2h4.html

[31] https://wiki.fysik.dtu.dk/gpaw/documentation/core.html

[32] https://wiki.fysik.dtu.dk/ase/

6.Appendix

6.1 Appendix A: Code for Fast Fourier Transform

```
ELEMENTAL FUNCTION isPowerOf2(n)
IMPLICIT NONE
INTEGER, INTENT (in) :: n
LOGICAL :: isPowerOf2
isPowerof2 = (n /= 0) .AND. (IAND(n,n-1) == 0)
END FUNCTION isPowerOf2
! the m-th fourier coefficient
RECURSIVE SUBROUTINE fft(m, f, C)
IMPLICIT NONE
INTEGER, INTENT (in) :: m
DOUBLE COMPLEX, INTENT (in) :: f(0:)
DOUBLE COMPLEX, INTENT (out) :: C
INTERFACE
FUNCTION isPowerOf2(n)
IMPLICIT NONE
INTEGER, INTENT (in) :: n
LOGICAL :: isPowerOf2
END FUNCTION isPowerOf2
END INTERFACE
INTEGER :: n
DOUBLE COMPLEX :: Ce, Co
DOUBLE COMPLEX :: a
DOUBLE PRECISION , PARAMETER :: pi = 3.14159265358979323846d0
n = SIZE(f)
IF (.NOT.isPowerof2(n)) STOP
IF (n == 1) THEN
C = f(0)
```

```
RETURN

END IF

CALL fft(m, f(0:n-1:2), Ce)

CALL fft(m, f(1:n-1:2), Co)

a = EXP(-2.d0 * pi * m * (0d0, 1.0d0) / n)

C = (Ce + a * Co) / 2d0

END SUBROUTINE fft

PROGRAM velocity

IMPLICIT NONE

INTEGER,PARAMETER :: N = 12              !arithmos atomon

INTEGER,PARAMETER :: N1 = N*3            !posa FFT tha ginoun

INTEGER,PARAMETER :: N2 = 100000         !arithmos run pou ginontai sto LAMMPS

INTEGER,PARAMETER :: N3 = 10             !kathe pote grafei sto data file

INTEGER,PARAMETER :: N4 = 2048           !posa simeia kratame sto FFT gia na einai
dynami tou 2

DOUBLE PRECISION,PARAMETER :: dt = 0.1d0   !se femtoseconds - time unit
=0.0001ps= 0.1fs

DOUBLE PRECISION,PARAMETER :: deltat = 1.0d-15 !se seconds - xroniko diastima
diadoxikon & simeion deltat=N3*dt

DOUBLE PRECISION,PARAMETER :: deltaf = 1.0d0/(N4*deltat)

DOUBLE PRECISION :: ja,xa,ya,za,a(1,3)        !diabazei id x y z kai bazei se pinaka ta vx vy
vz apo to data file

INTEGER :: i1,j1,j2,j3,j4,m,m1,m2,m3,m4,ts,t

DOUBLE PRECISION :: f(N1,N2/N3),freq

DOUBLE COMPLEX :: C, g(N1,N4)

REAL :: P(0:N4-1)

INTERFACE

SUBROUTINE fft(m, f, C)

IMPLICIT NONE

INTEGER, INTENT (in) :: m

DOUBLE COMPLEX, INTENT (in) :: f(0:)

DOUBLE COMPLEX, INTENT (out) :: C
```

```
END SUBROUTINE fft
END INTERFACE
OPEN(12,file="FFT_vel_new.data",action="read", status ="old")
OPEN(15,file="fft_frequency_P(m)_N=2048.txt",action="write", status ="replace")
j4 = 0
DO i1 = 1,N2/N3
j4 = j4 + 1
READ(12,*)
READ(12,*)ts ! timestep
t = ts*dt
DO j1 = 1,7
READ(12,*)
END DO
j3 = 0
DO j2 = 1,N
READ(12,*) ja,xa,ya,za,a(1,1),a(1,2),a(1,3)
j3 = j3 + 1
f(j3,j4) = a(1,1)
f(j3+1,j4) = a(1,2)
f(j3+2,j4) = a(1,3)
j3 = j3 + 2
END DO
END DO
DO m1 = 1,N1
m4 = 1
DO m2 = 7953,10000
g(m1,m4)=DCMPLX(f(m1,m2))
m4 = m4 + 1
END DO
END DO
P = 0
```

```
DO m3 = 0,N4-1

freq = m3*deltaf

DO m1 = 1,N1

CALL fft(m3,g(m1,:),C)

P(m3) = P(m3) + ABS(C)**2.0d0

END DO

WRITE(15,*)freq,freq*3.35641d-11, P(m3)

END DO

END PROGRAM velocity
```

6.2 Appendix B: Example of input script and data file for LAMMPS

Given below is an example of an input script used to perform simulations on LAMMPS. The simulation to be performed based on the example calls for a 100000 time step run starting from the file “data.NVT300Benzene”. Metal units are being used which uses picoseconds for time, Angstroms for length, Kelvin for temperature, bars for pressure, and eV for energy. The force field is set to the «rebo» potential. An NVT run is to be done with temperature rescaling to a desired temperature of 300K. The first dump file (pos_vel.data) will be created every 10 time steps and the positions and velocities of each atom will be calculated and written into the file. The second dump file (dump300NVT.*.xyz) stores the coordinates (x,y,z) of all atoms every 100 time steps.

```
units           metal
atom_style      atomic
boundary        p p p
read_data       data.NVT300Benzene
neighbor        0.5 bin
pair_style      rebo
pair_coeff      * * CH.rebo C H
variable        a equal 10
group           atoms12 id 1 2 3 4 5 6 7 8 9 10 11 12
dump            d3 atoms12 custom $a pos_vel.data id type x y z vx vy vz
velocity        all create 300.0 23456789
fix               1 all nvt temp 300.0 300.0 $(100.0*dt)
dump            d0 all xyz 100 dump300NVT.*.xyz
dump_modify     d0 element "C" "H"
thermo          10
```

thermo_style custom step cella cellb cellc pe temp

run 100000

Given below is an example of a data file. The simulation box size is set from -10 to 10 in the x,y, and z direction. The system contains 12 atoms of 2 atom types. The mass of the first atom type (named 1) is 12 g/mole and of the second atom type (named 2) is 1 g/mol. The x, y, and z coordinates of each atom is given. Apart from the coordinates, an id number is attached to each atom. The columns of 1 pertain to the atom type number and the molecule id.

LAMMPS Description

12 atoms

2 atom types

-10.0 10.0 xlo xhi

-10.0 10.0 ylo yhi

-10.0 10.0 zlo zhi

Masses

1 12.0

2 1.0

Atoms

1 1 1.38535 1.75416e-13 0

2 1 0.692676 1.19975 0

3 1 -0.692676 1.19975 0

4 1 -1.38535 1.79813e-13 0

5 1 -0.692676 -1.19975 0

6 1 0.692676 -1.19975 0

7 2 2.47547 5.33367e-15 0

8 2 1.23774 2.14382 0

9 2 -1.23774 2.14382 0

10 2 -2.47547 9.12684e-15 0

11 2 -1.23774 -2.14382 0

12 2 1.23774 -2.14382 0